UNIVERSITY OF CALIFORNIA
RIVERSIDE

The Cellular and Molecular Mechanism of Third Hand Cigarette Smoke-Induced Hepatic Steatosis

A Dissertation submitted in partial satisfaction
of the requirements for the degree of

Doctor of Philosophy

in

Cell, Molecular, and Developmental Biology

by

Cristina Flores

September 2017

Dissertation Committee:
Dr. Manuela Martins-Green, Chairperson
Dr. Frances Sladek
Dr. Margarita Curras-Collazo

The Dissertation of Cristina Flores is approved:

_____

_____

_____

Committee Chairperson

University of California, Riverside

Acknowledgments

I would like to give special thanks my advisor and chair of my dissertation committee, Manuela Martins-Green and my other committee members, Francis Sladek and Margarita Curras-Collazo, for the helpful comments and suggestions on my work. I would also like to thank Kathy Redd, Patricia Springer, and Morris Maduro for their help, advice and support for these past years. I would also like to give special thanks to Star Lee for all her teaching advice and all my students for allowing me to serve as their teaching assistant. I would also like to thank the undergraduate students in the laboratory for their help in cutting the material for the cages to be exposed to THS. Lastly, I'm very grateful to the Tobacco Related Disease Research Program for funding these studies.

Chapter 2 is modified from the published paper: Flores C, Adhami N, Martins-Green M (2016) THS Toxins Induce Hepatic Steatosis by Altering Oxidative Stress and SIRT1 Levels. J Clin Toxicol 6: 318; Chapter 3 is modified from the in press paper: Flores C, Adhami N, Martins-Green M (2017) The role of fatty acid metabolism and apolipoproteins in THS-induced hepatic steatosis in mice. J Clin Toxicol (*in press*).

Dedication

This dissertation is dedicated to people I truly admire and love. Thank you for all your love and inspiration.

ABSTRACT OF THE DISSERTATION

The Cellular and Molecular Mechanism of Third Hand Cigarette Smoke-induced hepatic steatosis.

by

Cristina Flores

Doctor of Philosophy, Graduate Program in Cell, Molecular and Developmental Biology
University of California, Riverside, September 2017
Dr. Manuela Martins-Green, Chairperson

Recent evidence indicates that third hand smoke (THS) is present mainly in places where smoking happens regularly but also in places where smoking has been banned but previously happened regularly. THS toxins remain in the contaminated surfaces, are re-emitted and have the ability to react with atmospheric gases to produce dangerous carcinogenic compounds. New evidence regarding the toxicity of THS continues to emerge and has been accumulating for the past 5 years. In order to investigate effects of THS toxins in the liver, I took a molecular and cellular approach by performing multiple cellular assays to study important cellular processes involved in lipid metabolism. The rodent model I used mimics human chronic exposure to THS and separates the effects of

SHS (second hand smoke) from THS. I also used different drug treatments and antioxidant treatments to modulate the effects of THS in mice and determine whether oxidative stress plays a key role in the development of THS-induced hepatic steatosis. Using this cellular and molecular approach, I was able to show that THS toxins alter the oxidative stress levels and increase oxidative-stress-mediated damage (protein damage, DNA damage and functional damage) in mice resulting in abnormal lipid metabolism. I was also able to show regulatory pathways, which involve regulators such as AMPK, SIRT1 and SREBP1c, are altered by THS toxins.

Furthermore, THS toxins alter fatty acid metabolism and lead to a decrease in VLDL assembly contributing to accumulation of lipids in the liver. THS-exposed mice have high levels of TG and fatty acids and less ATP production, suggesting these animals are less efficient metabolically compared to the control mice. AICAR treatment resulted in a decrease of fatty acids and TG levels, suggesting that increasing Sirtuin 3 (SIRT3), a key regulator of fatty acid metabolism results in less lipid accumulation in the liver. These findings provide evidence of the cellular and molecular basis of THS-induced hepatic steatosis in mice.

TABLE OF CONTENTS

List of Figures

Introduction

In 1881 James Bonsack invented the cigarette-making machine leading to the widespread smoking of cigarettes. For more than a century people have been smoking commercial cigarettes around the world resulting in many tobacco-related deaths each year. The adverse effects of smoking and second hand smoke (SHS) on human health have been shown via many research studies over the last decades. Only recently has the term third hand smoke (THS) been coined and introduced into the field of tobacco research. Third hand smoke is defined as the layer of tobacco toxin residues that accumulates on surfaces where smoking has occurred and/or continues to occur. THS has the following characteristics: (1) remains on surfaces; (2) re-emits into the gas phase; (3) reacts with other molecules present in the environment, resulting in the formation of carcinogens. Studies supporting the existence of THS have been accumulating over the last decade and have confirmed the presence of nicotine, one of the major components of THS, in the homes of smokers from various regional and socioeconomic demographics, suggesting exposure to toxins among different sectors of society. However, the effects of THS in human health have not been widely studied and the toxicity remains largely unknown.

Among the challenges that researchers face when studying the effects of THS in human health, is the low number of human subjects. Also, it is very difficult to control how many people smoke and consequently the exposure levels vary among subjects. Our lab has designed an *in vivo* system to study the systemic effects of long-term THS exposure using mice as the animal model. This system is ideal because of the following

reasons: (1) It differentiates between second hand smoke and THS; (2) one can perform controlled exposures; (3) it allows for the use of many animals so that statistical analysis can be performed.

In this document I start by reviewing what is currently known about THS toxicity (Chapter 1). Then I proceed to show molecular and cellular mechanisms of THS-induced hepatic steatosis (Chapter 2). Subsequently, I discuss the role of THS-exposure on fatty acid metabolism and on lipoproteins in hepatic steatosis (Chapter 3). Lastly, I conclude by summarizing the findings and discussing the implications of our findings for liver health (Chapter 4).

CHAPTER 1:
A brief overview of the effects of THS in human health

Cigarette toxins are detrimental to human health because these toxins affect a wide variety of biological processes. The smoke is divided into active SHS and passive THS. SHS and THS co-exist initially when THS is starting to form from the tobacco toxins. Unlike SHS that is visible, THS is invisible and consequently the characterization of THS toxins is not yet fully developed. Unlike SHS exposure, which occurs in low intervals at high dose mainly via inhalation, the exposure to THS exposure is slow and at low dose for prolonged periods and can occur via inhalation, ingestion and dermal uptake. These toxins can remain on these surfaces for days or months. If the exposure to THS is chronic, multiple layers of toxins build up continuously making these surfaces very toxic. These toxins age with time, becoming progressively more reactive and toxic. THS toxins have the ability be re-emitted and react with other gaseous compounds found in the atmosphere and lead to the formation of tobacco specific N-nitrosamines (TSNA) such as 1-(N-methyl-N-nitrosamino)-1-(2-pyridinyl)-4- butanal (NNA), 4-(methylnitrosamino)-1-(3-pyridinyl)-1-buta- none (NNK) and N-nitroso nornicotine (NNN). These chemicals are carcinogens. Two specific TSNA, NNA and NNK have been shown to result in genotoxicity and result in DNA damage. *In vivo* and *in vitro* studies have been done to study the effects of THS in human health. Multiple epidemiological studies have shown the presence of chemical metabolites in the urine of children who live in the houses of smokers. The chemical metabolites also have been found in the homes of families who reported no indoor smoking. It is now known that THS exposure results in chemical assimilation but the repercussions of this exposure still remain to be elucidated. Recent studies also showed that THS exposure leads to abnormal

cognitive functions in children and DNA damage in human cells [1-2]. Mice exposed to THS toxins also show higher levels of hyperactivity compared to mice that are not exposed to THS.

In recent years, the effects of third hand smoke (THS) in human health have been investigated using different experimental approaches ranging from epidemiological toxicological studies to biological studies. Epidemiological and toxicological studies showed THS toxins remained, were reemitted and reacted with atmospheric gasses leading to the formation of carcinogenic compounds leading to additional research studies [3-9]. These studies also showed that THS toxins could be absorbed, metabolized and excreted in the urine [10-12]. Using cell lines, researchers have been able to show THS exposure results in DNA damage and changes in gene expression *in vitro* [13-20]. The animal studies have provided more insights into the effect of THS toxins in immunity and metabolism [21-22]. In this chapter, I discuss a brief overview of the research progress in the field of THS with a specific focus on the studies that have investigated the effects of THS exposure in human health.

THS exposure in epidemiological human studies

The amount of evidence of the toxicity of third hand smoke has been accumulating over the past decades. Children are among the populations more susceptible to toxicity of THS since they spend more time indoors and continue to develop through their childhood. Children also have the tendency to crawl and touch contaminated

surfaces more frequently than adults; consequently they come into close contact with THS toxins more often.

In a recent study, Matt et al. was able to show that nicotine levels were higher in the houses of smokers than nonsmokers and that nicotine metabolites were higher in children living in houses of smokes than nonsmokers [3]. By measuring the (4-(methylnitrosamino)-1-(3-pyridyl)-1-butanol) (NNAL)/cotinine concentrations in infants' urine, the researchers were able to show neonatal intensive care units are contaminated with THS toxins [12]. In another study, Ramirez et al. measured the nicotine and nitrosamines/TSNAs levels in household samples and found the cancer risk for children increased [13]. Some of the THS toxins can act as neurotoxic and low levels of prenatal exposure results in cognitive deficits in infants [1].

THS exposure results in genotoxicity in cell models

THS contains many toxic compounds, which include mutagens and carcinogens resulting in genotoxicity. Genotoxicity is one of the critical mechanisms responsible for many types of cancer caused by active smoking and SHS exposure. The ability of THS to alter the genome integrity of humans was not well known but recent research studies have been done to access the genotoxic potential of THS toxins. The main finding of these studies is summarized below.

In a recent study, significant increases in DNA strand breaks were observed in human liver cancer cells (HepG2) exposed to THS [15]. They discovered both acute and chronic exposure of materials to THS-induced DNA strand breaks, suggesting that THS

toxins are genotoxic because double strand breaks (DSB) are the most dangerous form of DNA damage. Another study demonstrated that when epithelial cells (BEAS-2B) were exposed to THS toxins, double strand breaks formed. Interestingly, the amount of DSB formed was similar to the amount of DSB induced by SHS [16]. Other studies have investigated the effect of specific THS constituents, such as NNK and NNA, on DNA stability and have shown increasing the dose exposure of these toxins leads to DNA damage [16-17]. Low amounts of 0.01 to 100 μM of NNA resulted in DSB in HepG2 cells [16].

THS exposure results in metabolic changes in male cell line

Recent studies have shown THS exposure alters the metabolome of cell lines suggesting the ability of THS toxins to alter the metabolism of these specific cell lines. Chronic exposure of GC-2 and TM-4, two rodent cell lines, resulted in changes in cell cycle, apoptosis, reactive oxygen and glutathione metabolism in GC2 whereas in TM-4, ammonia metabolism was altered [20]. In this study, using RT-PCR analyses, they were able to show that enzymes involved in glutathione, nucleic acids and ammonia metabolism, were changed.

THS exposure results in changes in body mass and immunity in mice

Some studies have been done accessing the health threat of THS to infants and young children who are in smokers' homes and discovered that the damage that occurs at early stages may continue in adulthood. In this study, they exposed C57BL/6J mice to THS and investigated the effects of THS exposure on body mass and blood cell

population from birth until weaning (21 days old). Both THS-exposed female and THS-exposed male mice had a significant reduction in weight gain compared to the non-exposed mice. However, the effect of THS on body mass was diminished after the mice were placed in a non-exposed setting. The THS-exposed mice displayed similar body mass to the control mice at 5, 8, 12 weeks [21].

THS exposure during the first 3 weeks of life altered the immunity in the THS-exposed mice. THS exposure resulted in an increase of eosinophil number in blood circulation in both genders at 17 weeks of age. The-exposed male mice also had a significant increase in basophil levels and THS-exposed mice had increased neutrophils. Fluorescence-activated cell sorting (FACS) analysis in the blood of these mice also showed THS exposure results in a significantly increased percentage of B-cells and T-suppressor cells, with a decreased percentage of myeloid cells in adult rats [18]. Taken together these findings suggest early exposure to THS results in cellular damage and that this damage can persist into adulthood.

THS exposure results in changes in metabolic and behavioral changes in mice

The studies summarized above focused on dose-dependent damage and acute exposure. Studies investigating the effects of long-term exposure have also been performed in our laboratory to study the effects of THS in different organs. These studies were done and are being done using a rodent model, which separates the effects of SHS from THS exposure and mimics the exposure of THS toxins in humans. The mice live in

cages of exposed material (10g curtain, 10g carpet and 10g upholstery) for six months before specific analyses are done (**Figure 1.1**). The materials are exposed to THS toxins using a smoking machine (Teague Enterprises, Inc., Woodland, CA) and two packs of 3R4F research cigarettes are smoked each day, 5 days/week [23-24]. After six months of expose the effects of THS toxins in specific organs and behavior are investigated and the main findings are summarized below (**Figure 1.2**).

THS exposure results in inflammation and fibrosis in the lung of mice

Exposure to THS-toxins for six months resulted in an increase of leukocyte infiltration to respiratory bronchioles suggesting chronic exposure to THS toxins leads to inflammation in the lung. The alveoli of the THS-exposed mice were also disrupted and high amounts of disorganized collagen fibers were present in the lung tissue indicating fibrosis [22]. Taken together these findings suggested that THS exposure could result in the development of lung fibrosis in mice.

THS exposure results in altered behavior in mice

Chronic exposure to THS-toxins results in hyperactivity in THS-exposed mice. An Open Field test analysis of these animals showed that mice exposed to THS toxins had the tendency to move more than the control and transition less between behaviors (walking, stationary or rearing). Consequently THS-exposed mice covered longer lengths

at higher speeds of movement than the control mice. THS-exposed mice also had the tendency to stay in the periphery more than the control mice. Taken together, the open field analysis indicated that THS toxins have the ability to alter the behavior and result in hyperactivity in mice.

THS exposure result in abnormal lipid and glucose metabolism in mice

Chronic exposure to THS toxins results in abnormal lipid metabolism in the liver. THS-exposed mice accumulated higher levels of lipids in the liver resulting in hepatic steatosis in male mice. Histological analysis of liver tissue of THS-exposed mice showed that these mice had larger lipid droplets compared to the control [22]. Circulating triglycerides (TG) and low-density lipoprotein (LDL) were also elevated whereas high-density lipoprotein (HDL) was decreased in THS-exposed mice compared to the control. Elevated levels of TG and LDL have been associated with metabolic syndrome and cardiovascular diseases [25-35]. Therefore, THS-exposed mice seem to be predisposed to cardiovascular diseases and type 2 diabetes [22]. Exposure to THS-toxins resulted in pre-diabetic phenotype in THS-exposed mice. These animals had elevated fasting glucose compared to the control. THS exposed mice were unable to metabolize glucose or use insulin efficiently when challenged with glucose using the IPTG test or insulin (IIT) test. Taken together, these findings suggested that chronic exposure to THS toxins has the ability to induce hepatic steatosis in mice. These findings have a significant clinical relevance because smoking has been linked to abnormal glucose metabolism in humans in previous studies [36-42].

Summary and conclusions

Evidence is mounting for the past seven years that THS toxins are damaging to the body. Epidemiological, toxicological, in-vitro and animal research studies have demonstrated that THS exposure can have detrimental effects in human health (**Figure 1.3**). More specifically, this evidence has demonstrated THS toxins have the ability to alter the following: (1) DNA integrity (2) behavior (3) metabolism and (4) immunity. The mechanism for which this cellular and molecular damage occurs is not yet fully understood and additional studies need to be done to elucidate how THS-toxins can induce this damage.

References

1. Yolton, K.; Khoury, J.; Xu, Y.; Succop, P.; Lanphear, B.; Bernert, J.T.; Lester, B. Low level prenatal exposure to nicotine and infant neurobehavior. *Neurotoxicol. Teratol.* 2009, *31*, 356–363.

2. Hang, B.; Sarker, A.H.; Havel, C.; Saha, S.; Hazra, T.K.; Schick, S.; Jacob, P., III; Rehan, V.K.; Chenna, A.; Sharan, D.; et al. Thirdhand smoke causes DNA damage in human cells. *Mutagenesis.* 2013, *28*, 381–391.

3. Matt, G.E.; Quintana, P.J.; Zakarian, J.M.; Fortmann, A.L.; Chatfield, D.A.; Hoh, E.; Uribe, A.M.; Hovell, M.F. When smokers move out and non-smokers move in: Residential thirdhand smoke pollution and exposure. *Tob. Control.* 2011, *20*.

4. Matt, G. E., Quintana, P., Zakarian, J., Hoh, E., Hovell, M. F., Mahabee-Gittens, M., and Chatfield, D. (2016) When Smokers Quit: Exposure to Nicotine and Carcinogen Persists from Thirdhand Smoke Population [In Press]. Tobacco Control, DOI: 10.1136/tobaccocontrol- 2016-053119.

5. Sleiman M, Gundel L, Pankow J, Jacob P, Singer B, Hugo D. Formation of carcinogens indoors by surface-mediated reactions of nicotine with nitrous acid, leading to potential thirdhand smoke hazards. Proc. Natl. Acad. Sci.2010; 107: 6576–6581

6. Sleiman, M., Destaillats, H., Smith, J. D., Liu, C.-L., Ahmed, M., Wilson, K. R., and Gundel, L. A. (2010) Secondary organic aerosol formation from ozone-initiated reactions with nicotine and second- hand tobacco smoke. Atmos. Environ. 44, 4191−4198.

7. Hecht, S. S., Chen, C.-H. B., Ornaf, R. M., Jacobs, E., Adams, J. D., and Hoffmann, D. (1978) Chemical studies on tobacco smoke. 52. Reaction of nicotine and sodium nitrite: formation of nitrosamines and fragmentation of the pyrrolidine ring. J. Org. Chem. 43, 72−76.

8. Schick, S. F., Farraro, K. F., Perrino, C., Sleiman, M., van de Vossenberg, G., Trinh, M. P., Hammond, S. K., Jenkins, B. M., and Balmes, J. (2014) Thirdhand cigarette smoke in an experimental chamber: evidence of surface deposition of nicotine, nitrosamines and polycyclic aromatic hydrocarbons and de novo formation of NNK. Tob Control 23, 152−9.

9. Whitehead, T. P., Havel, C., Metayer, C., Benowitz, N. L., and Jacob, P., 3rd

(2015) Tobacco alkaloids and tobacco-specific nitrosamines in dust from homes of smokeless tobacco users, active smokers, and nontobacco users. Chem. Res. Toxicol. 28, 1007−14.

10. Hecht S, Carmella S, Le K. 4-(Methylnitrosamino)-1-(3-Pyridyl)-1-Butanol and its Glucuronides in the Urine of Infants Exposed to Environmental Tobacco Smoke.Cancer Epidemiol Biomarkers Prev. 2006; 15:988–992.

11. Matt, G. E., Quintana, P. J. E., Hovell, M. F., Bernert, J. T., Song, S., Novianti, N., Juarez, T., Floro, J., Gehrman, C., Garcia, M., and Larson, S. (2004) Households contaminated by environmental tobacco smoke: sources of infant exposures. Tobacco Control 13, 29−37.

12. Northrup, T.F.; Khan, A.M.; Jacob, P., III; Benowitz, N.L.; Hoh, E.; Hovell, M.F.; Matt, G.E.; Stotts, A.L. Thirdhand smoke contamination in hospital settings: Assessing exposure risk for vulnerable paediatric patients. *Tob. Control.* 2015, *25*.

13. Ramirez, N.; Ozel, M.Z.; Lewis, A.C.; Marce, R.M.; Borrull, F.; Hamilton, J.F. Exposure to nitrosamines in thirdhand tobacco smoke increases cancer risk in non-smokers. *Environ. Int.* 2014, *71*, 139–147.

14. Hang, B. (2010) Formation and Repair of Tobacco Carcinogen- Derived Bulky DNA Adducts. J. Nucleic Acids 2010, 1−29.

15. Yu, R., Wu, M., Lin, S., and Talbot, P. (2006) Cigarette Smoke Toxicants Alter Growth and Survival of Cultured Mammalian Cells. Toxicol. Sci. 93, 82−95.

16. Hang, B.; Lavarone, A.; Havel, C.; Jacob, P., III; Villalta, P.; Matter, B.; Sharan, D.; Hang, M.; Sleiman, M.; Destaillats, H.; et al. NNA, a Thirdhand Smoke Constituent, Induces DNA Damage in Vitro and in Human Cells. In Proceedings of the 247th National Meeting of the American Chemical Society (ACS) with Press Release, Dallas, TX, USA, 14–19 March 2014; American Chemical Society: Washington, DC, USA, 2014.

17. Santos, J.H.; Meyer, J.N.; Mandavilli, B.S.; van Houten, B. Quantitative PCR-based measurement of nuclear and mitochondrial DNA damage and repair in mammalian cells. *Methods Mol. Biol.* 2006, *314*, 183–199.

18. Lao, Y.; Yu, N.; Kassie, F.; Villalta, P.W.; Hecht, S.S. Formation and accumulation of pyridyloxobutyl DNA adducts in F344 rats chronically treated with 4-(methylnitrosamino)-1-(3-pyridyl)-1-butanone and enantiomers of its metabolite, 4-(methylnitrosamino)-1-(3-pyridyl)-1-butanol. *Chem. Res. Toxicol.* 2007, *20*, 235–245.

19. Bahl, V.; Johnson, K.; Phandthong, R.; Zahedi, A.; Schick, S.F.; Talbot, P. Thirdhand cigarette smoke causes stress-induced mitochondrial hyperfusion and alters the transcriptional profile of stem cells. *Toxicol. Sci.* 2016, *153*, 55–69.

20. Xu, B.; Chen, M.; Yao, M.; Ji, X.; Mao, Z.; Tang, W.; Qiao, S.; Schick, S.F.; Mao, J.H.; Hang, B.; et al. Metabolomics reveals metabolic changes in male reproductive cells exposed to thirdhand smoke. *Sci. Rep.* 2015, *5*, 15512.

21. Hang, B.; Snijders, A.M.; Huang, Y.; Schick, S.F.; Wang, P.; Xia, Y.; Havel, C.; Jacob, P., III; Benowitz, N.; Destaillats, H.; et al. Early exposure to thirdhand cigarette smoke affects body mass and the development of immunity in mice. *Sci. Rep.* 2017, *7*, 41915.

22. Martins-Green, M.; Adhami, N.; Frankos, M.; Valdez, M.; Goodwin, B.; Lyubovitsky, J.; Dhall, S.; Garcia, M.; Egiebor, I.; Martinez, B.; et al. Cigarette smoke toxins deposited on surfaces: Implications for human health. *PLoS ONE* 2014, *9*, e86391.

23. Teague-Enterprises Inhalation exposure apparatus, available at: http://www.teague-ent.com/equipment/smoking-machines http:// www.teague-ent.com/equipment/smoking-machines (July 1, 2017).

24. NIH The FTC Cigarette Test Method for Determining Tar, Nicotine, and Carbon Monoxide Yields of U.S. Cigarettes. http://cancercontrol.cancer.gov/brp/TCRB/monographs/7/.

25. Kisfali, P., Polgar, N., Safrany, E., Sumegi, K., Melegh, B. I., Bene, J., Weber, A., Hetyesy, K., and Melegh, B. (2010) Triglyceride level affecting shared susceptibility genes in metabolic syndrome and coronary artery disease. Curr. Med. Chem. 17 (30), 3533−41.

26. Tsai C-H, Li T-C, Lin C-C. Metabolic Syndrome as a Risk Factor for Nonalcoholic Fatty Liver Disease. South Med J. 2008;101:900–905.

27. Targher G, Bertolini L, Padovani R, et al. Prevalence of Nonalcoholic Fatty Liver Disease and Its Association with Cardiovascular Disease among Type 2 Diabetic Patients. Diabetes Care. 2007;30:1212–1218.

28. Ua A, Sa T, Sa B, et al. Association between nonalcoholic fatty liver disease and coronary artery disease. Coronary Artery Dis. 2007;18:433–436.

29. Pacifico L, Cantisani V, Ricci P, et al. Nonalcoholic fatty liver disease and carotid atherosclerosis in children. Pediatr Res. 2008;63:423–427.

30. Brea A, Mosquera D, Martin E, et al. Nonalcoholic Fatty Liver Disease Is Associated With Carotid Atherosclerosis: A Case-Control Study. Arterioscler Thromb Vasc Biol. 2005;25:1045–1050.

31. Targher G, Bertolini L, Padovani R, et al. Relation of Nonalcoholic Hepatic Steatosis to Early Carotid Atherosclerosis in Healthy Men: Role of visceral fat accumulation. Diabetes Care. 2004;27:2498–2500.

32. Sookoian S, Pirola CJ. Non-alcoholic fatty liver disease is strongly associated with carotid atherosclerosis: A systematic review. J Hepatol. 2008;49:600–607.

33. Volzke H, Robinson DM, Kleine V, et al. Hepatic steatosis is associated with an increased risk of carotid atherosclerosis. World Journal of Gastroenterology. 2005;11:1848–1853.

34. Adhami, N., Starck, S. R., Flores, C., and Martins Green, M. (2016) A health threat to bystanders living in the homes of smokers: how smoke toxins deposited on surfaces can cause insulin resistance. PLoS One 11, e0149510.

35. Matsuki H, Hashimoto K, Arashidani K, Akiyama Y, Amagai T. Studies on a simultaneous analytical method of urinary nicotine and its metabolites, and their half-lives in urine. J UOEH. 2008; 30: 235– 252. PMID: 18783007

36. Willi C, Bodenmann P, Ghali W, Faris P, Cornuz J. Active smoking and the risk of type 2 diabetes in infants and children: a systematic review and meta-analysis. JAMA. 2007; 298:2654–2664. PMID: 18073361

37. Royal College of Physicians. Passive smoking and children. A report of the

Tobacco Advisory Group of the Royal College of Physicians. 2010 London: Royal College of Physicians.

38. Shoelson S, Lee J, Goldfine A. Inflammation and insulin resistance. The Journal of Clinical Investigation. 1995; 116: 1793–1801.

39. Frati A, Iniestra F, Raul C. Acute effect of cigarette smoking on glucose tolerance and other cardiovascular risk factors. Diabetes Care. 1996; 19:112–118. PMID: 8718429

40. Theiring E,Brüske C, Kratzsch J, Thiery J, Sausenthale S, Meisinger C, et al.Prenatal And Postnatal Exposure To Environmental Tobacco Smoke And Development Of Insulin Resistance In 10 Year Old Children. International Journal of Hygiene and Environmental Health. 2011; 214 [5]: 361–368 doi: 10. 1016/j.ijheh.2011.04.004 PMID: 21570350 .

41. Attvall S, Fowelin J, Lager I, VonSchenck H, Smith H. Smoking induces insulin resistance: a potential link with the insulin resistance syndrome. J Intern Med. 1993; 223:327–332.

42. Zhang L, Curhan G, Hu F, Rimm E, Forman J. Association between passive and active smoking and incident type 2 diabetes in women. Diabetes care. 2011; 34[4]:892–7.

Figure 1.1 Schematic of long term THS exposure using mice model. Mice (3 weeks of age) are exposed to THS toxins for six months. Common household material (10g carpet, 10g cotton and 10g upholstery) is exposed to THS toxins a Teague Smoke Machine that mimics a interment smoker (2 packs of cigarettes each day for 5 days).

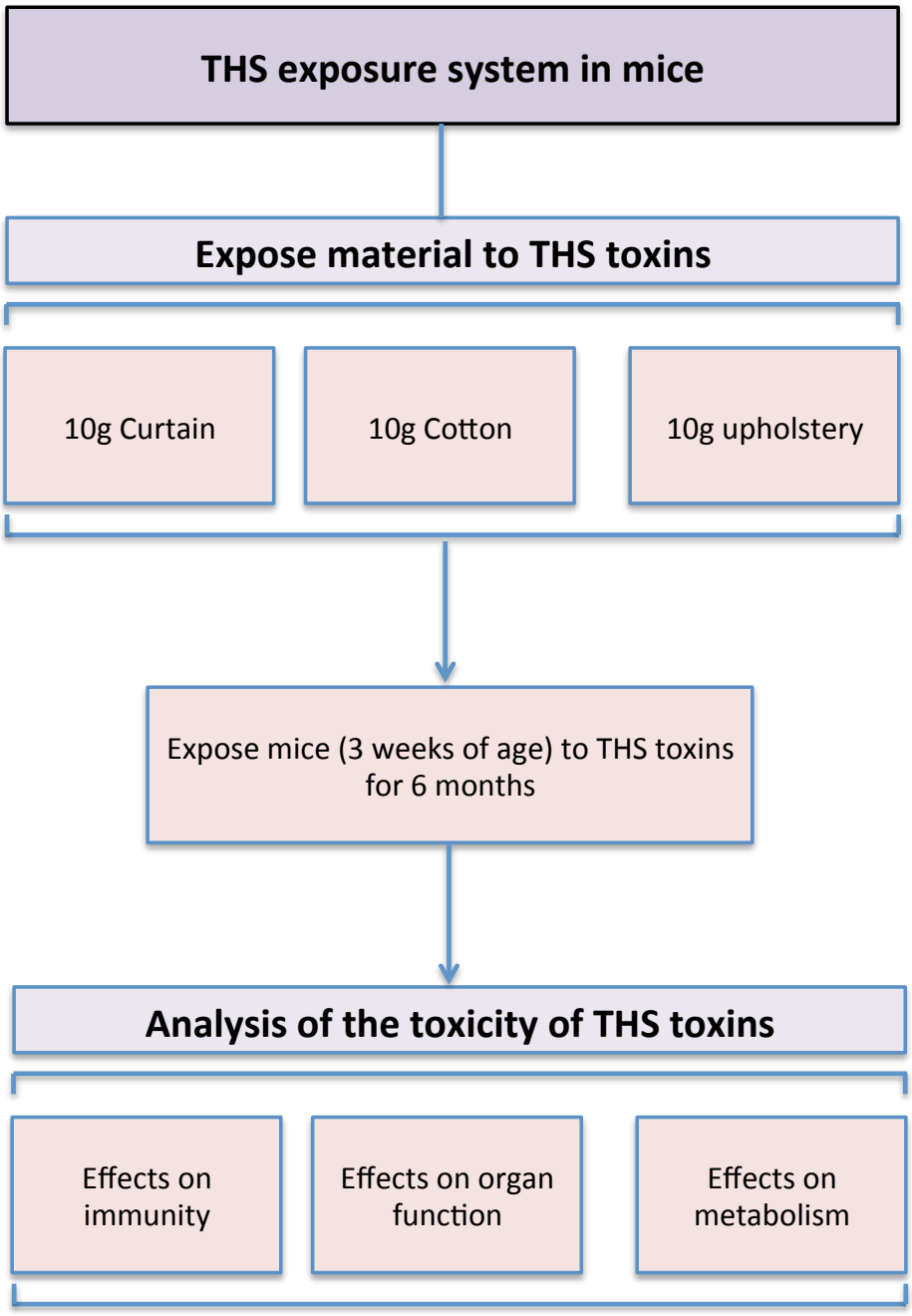
THS exposure system in mice
Expose material to THS toxins
10g Curtain
10g Cotton
10g upholstery
Expose mice (3 weeks of age) to THS toxins for 6 months
Analysis of the toxicity of THS toxins
Effects on immunity
Effects on organ function
Effects on metabolism

Figure 1.1

Figure 1.2 Summary of major findings using mice model to study the long-term effects of THS toxins in different organs and behavior. THS exposure results in changes in behavior, lung damage, lipid accumulation in the liver and altered glucose and lipid metabolism in mice.

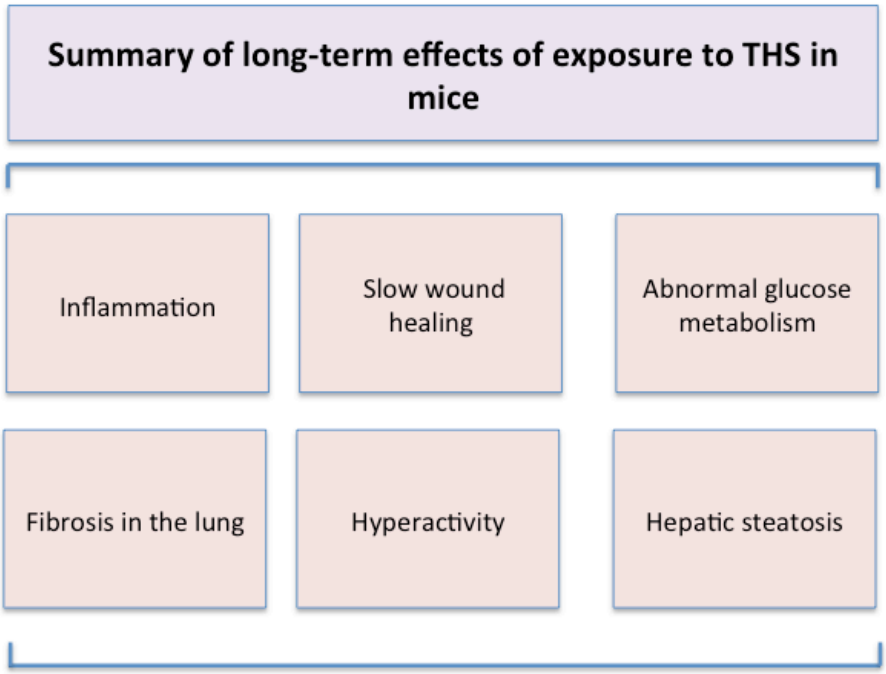
Summary of long-term effects of exposure to THS in mice
Inflammation
Slow wound healing
Abnormal glucose metabolism
Fibrosis in the lung
Hyperactivity
Hepatic steatosis

Figure 1.2

Figure 1.3 Summary of the effects of THS on human health. THS toxins results in DNA damage, changes in metabolism, changes in immunity and altered behavior in mice.

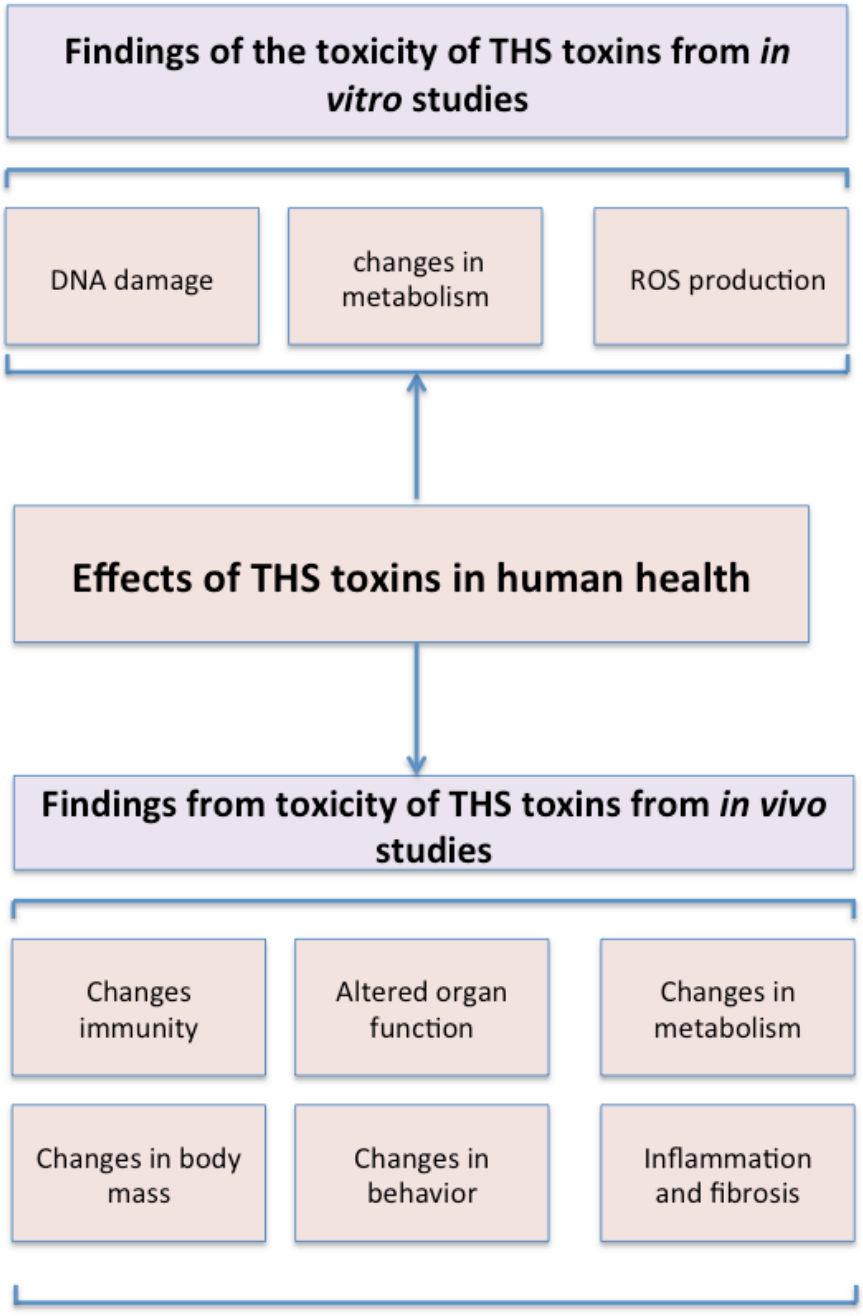
Findings of the toxicity of THS toxins from *in vitro* studies
DNA damage
changes in metabolism
ROS production
Effects of THS toxins in human health
Findings from toxicity of THS toxins from *in vivo* studies
Changes immunity
Altered organ function
Changes in metabolism
Changes in body mass
Changes in behavior
Inflammation and fibrosis

Figure 1.3

CHAPTER 2:
Cellular and Molecular mechanism of THS-induced hepatic steatosis

Abstract

Background: Third hand smoke (THS) forms when second hand smoke (SHS) tobacco toxins accumulate on surfaces such as walls, carpets and clothing and can result in adverse health effects.

Objective: This study was designed to investigate the mechanism of THS-induced hepatic steatosis.

Methodology: We used an *in vivo* exposure system that mimics exposure of humans to THS to investigate the effects of THS on hepatic lipid metabolism. THS-exposed mice were treated either with the liver-damaging drug, N-acetyl-p-aminophenol (APAP/Tylenol) to increase oxidative stress or with the antioxidants N-acetyl-cysteine and α-Tocopherol which decrease oxidative stress.

Results: THS-exposed mice have higher levels of superoxide dismutase activity and H_2O_2 levels. However, no significant changes in activity of the antioxidant enzymes catalase and glutathione peroxidase were found, implying the presence of high levels of hydrogen peroxide in the liver. Furthermore, THS-exposed mice also have a lower $NADP^+$/NADPH ratio, indicating decreased ability of these mice to combat oxidative stress. THS-exposed mice show a decrease in ATP production, increase in aspartate aminotransferase (AST) activity, as well as increased molecular damage (lipid peroxidation, protein nitrosylation and DNA damage). Treating THS- exposed mice with APAP/Tylenol enhances the THS-induced damage whereas treating with antioxidants reduces the damage. THS-exposed mice also have lower sirtuin 1 (SIRT1) levels compared to controls which decreased activation of 5' AMP-activated protein kinase (AMPK) and increased sterol regulatory element binding protein 1c (SREBP1c).

Conclusion: THS-exposed mice on a normal diet have increased oxidative stress and damage mediated by oxidative stress, which results in alterations to the SIRT1/AMPK/SREPB1c signaling pathway. Increasing oxidative stress results in enhanced THS-induced damage whereas decreasing oxidative stress causes improvement in the THS-induced liver damage. Our results show that THS is a new risk factor contributing to the development of liver steatosis and highlight the danger of THS in general.

Introduction

Cigarette toxins are detrimental to human health; these toxins affect a wide variety of biological processes. The cigarette toxins are initially emitted when the smoker exhales the smoke of the cigarette into the air as mainstream second hand smoke (SHS); these toxins will then transform physically and chemically, giving rise to third hand smoke (THS). SHS smoke is the smoke that is inhaled and exhaled by the smoker and by a by-stander directly. The exposure frequency of SHS is short intervals at very high dosage and then, with time, SHS toxins dissipate and are removed by ventilation. However, SHS has been shown to be very dangerous to non smokers and numerous studies have shown its effects in human health [1-2]. Second hand smoke contains more than 4000 chemicals, which include ammonia, carbon monoxide and sulfur dioxide [1-2]. There is a strong correlation between second hand smoke and lung cancer in both the smoker and non-smoker [2]. Some studies have highlighted the dangers of second hand smoke to non smokers by showing it results in 50, 000 deaths per year [2]. The effects of SHS have been widely studied and many publications have addressed the damage of SHS toxins in multiple organs via oxidative stress [3-9].

Third hand smoke (THS) forms when second hand smoke (SHS) tobacco toxins accumulate on surfaces such as walls, carpets and clothing [10-13]. Moreover, these toxins have the ability to react with gases in the air, such as nitrous acid, and produce dangerous carcinogens [14-18]. Individuals are exposed to THS toxins when they come into contact with the deposited toxins or when the toxins are re-emitted into the air. Exposure to THS toxins can result in detrimental health outcomes in individuals who are

chronically exposed to them [19-26]. These health effects vary from metabolic disorders to cognitive perturbations. Children are one of the sectors of the population that is most susceptible to tobacco toxins and studies have shown that tobacco metabolites are detected in their urine [22-24]. Unfortunately, this dangerous exposure continues. In 2007, about 5.5 million children lived in households where someone smoked inside the home [21]. Even in households where indoor smoking was not reported, the tobacco metabolites could still be detected in the children's urine [22-25].

Studies *in vitro* have shown that THS is toxic to human cells. When a liver cell line, HepG2 cells, was exposed to THS toxins their DNA integrity and stability was compromised [25]. Both acute and chronic THS exposure resulted in double strand DNA breaks [25]. These investigators also showed that the molecular damage observed in HepG2 cells was associated with the increase in cellular oxidative stress and therefore suggested that oxidative stress is a major contributor to THS-mediated toxicity *in vitro* [25]. Another *in vitro* study focused on the effects of THS in the development of the lung using fetal rat lung explants [26]. These investigators showed that when fetal rat lungs were exposed to the THS toxins nicotine, 1-(N-methyl-N-nitrosamino)-1-(3-pyridinyl)-4butanal (NNA), or 4-(methylnitrosamino)-1-(3-pyridyl)-1-butanone (NNK), there was a disruption in the development of alveolar interstitial fibroblasts and that the disruption occurred via down regulation of PPAR-γ signaling [26]. PPAR-γ signaling controls alveolar development and down regulation of this signaling in the lungs suggested a disruption in alveolar epithelial-mesenchymal paracrine signaling, which prevents normal lung development. Exposure to THS toxins also resulted in increase of fibronectin and

calponin protein levels as well as increase in apoptosis, which are markers for abnormal lung development. Together these findings suggest that the lungs of rats exposed to THS toxins do not develop normally, highlighting the danger of exposure to these toxins during lung development.

It also has been shown that THS toxins have the ability to cause metabolic changes in two male germ cell lines [27]. When spermatogonia (GC-2) and sertoli derived cells (TM-4) were exposed to THS toxins for 24 hours, the investigators observed changes in metabolic enzymes involved in glutathione, ammonia and nucleic acid metabolism [27]. In GC-2 cells, THS exposure resulted in increase in synthesis and decrease in the breakdown of GSH. GSH is a major component of the antioxidant defense pathway and these findings suggest spermatogonia might use this enzyme to combat the high levels of oxidative stress [27]. In TM-4 cells, there are increased metabolites involved in nucleic acid metabolism, suggesting that THS toxins are genotoxic and have the ability to compromise the integrity of genetic material [27]. THS exposure did not have effects on cell viability, cell cycle or apoptosis in these two male germ cell lines [27]. However, this in *vitro* study highlighted the sensitivity of male germ cells to THS toxins.

In addition to the findings *in vitro*, the detrimental effects of THS toxins have also been shown to alter human behavior. Epidemiological studies have shown that THS exposure results in abnormal cognitive function in children [28]. Children exposed to THS toxins are more hyperactive than children that live in environments with less THS contamination. Also, children are exposed to higher levels of these toxins than adults

because they are in closer contact with the contaminated surfaces, lick their fingers and their surface-to-volume ratio is larger [28-29]. In addition, they are also more susceptible because their liver is not fully developed and therefore is not as effective in detoxification of toxins. Also, smoking during pregnancy or after pregnancy is dangerous for the developing fetus and results in impaired lung function [30-31]. Post-natal exposure to THS toxins also results in increased problems with the larynx, trachea and bronchi. This resulted in increased cough-and-asthma related symptoms in these children, suggesting THS toxins are detrimental for lung health of children living in homes contaminated with THS toxins.

We have developed an *in vivo* THS exposure system of mice that mimics THS exposure in humans [32]. Our model is a novel exposure system that allows us to study the effects of long-term THS exposure in different organs of male C57BL/6 mice. Using this exposure method, we have shown that THS exposure leads to lipid accumulation in the liver of these mice, suggesting that they have abnormal metabolism and insulin resistance [32-33]. These findings suggest that THS exposure is a new risk for hepatic steatosis.

Hepatic steatosis is the earliest stage of and a hallmark of non-alcoholic liver disease (NAFLD), which is the most common liver disease worldwide [34-35]. In some patients, steatosis can progress into fibrosis and then to cirrhosis if is not treated early. In the U.S., the prevalence of NAFLD is estimated to be around 20% in the general population and the percentage quadruples in morbidly obese individuals [34-35]. NAFLD is not limited to adults; the incidence of NAFLD among the pediatric population is

increasing and it is estimated to account for about 14% of all NAFLD cases [34-35]. NAFLD is a complex process that results from metabolic abnormalities [36-37]. Many patients show dyslipidemia, malfunction of beta oxidative enzymes, deficiency in lipoproteins, and immune dysregulation [38-39]. Obesity, metabolic disorders, drugs or smoking are some of the major risk factors contributing to the development of NAFLD [40-42]. This disease is primarily controlled through changes in life-style, cessation of chemical exposure or antioxidant treatments [43-45].

In this study, we performed cellular and molecular studies to investigate whether THS exposure leads to increased oxidative stress in liver, leading to abnormal lipid metabolism and resulting in hepatic steatosis. Here, we show that mice exposed to THS toxins have altered oxidative stress in the liver. Increasing oxidative stress by treating the mice with N-acetyl-p-aminophenol (APAP/tylenol) leads to exacerbation of THS-induce hepatic steatosis whereas antioxidant treatment ameliorates this condition. These findings suggest that oxidative stress caused by THS toxins leads to lipid accumulation in the liver. More specifically, THS toxins alter the SIRT1/AMPK/SREPB1c pathway, which regulates lipid metabolism in the liver, suggesting, that THS toxins are a new risk factor for development of hepatic steatosis.

Materials and methods

Animals: Male C57BL/6 mice were divided into control and experimental groups (THS-exposed mice). The experimental group was exposed to THS toxins after weaning for 24 weeks. The control group was never exposed to THS toxins. Both control and THS-exposed mice were maintained under controlled environmental conditions -- 12-hr light/dark cycle in conventional cages with *ad libitum* access to standard chow (percent calories: 58% carbohydrate, 28.5% protein, and 13.5% fat) and water.

Ethics Statement: All animal experimental protocols were approved by the University of California, Riverside, Institutional Animal Care and Use Committee (UCR-IACUC). Mice were euthanized by carbon dioxide (CO_2) inhalation, which is the most common method of euthanasia used by NIH. The amount and length of CO_2 exposure were approved by UCR-IACUC.

THS exposure method: Common household fabrics such as curtain material, upholstery and carpet were placed in empty mouse cages and exposed to SHS generated by the a Teague smoking machine as previously described in [32]. Each cage contained 10 g of curtain material (cotton) 10 g of upholstery (cotton and fiber) and two $16in^2$ pieces of carpet (fiber) to maintain equal exposure levels across all experimental groups. Two packs of 3R4F research cigarettes were smoked each day, five days per week to mimic an intermittent smoker. The smoke was routed to a mixing compartment to mix with air and

the mixture distributed between two exposure chambers, each containing eight cages with the materials. The gravimetric method was used to determine the total particulate concentrations in each smoke chamber. The weight of Whatman grade 40 quantitative cellulose filter papers was recorded before introducing the filter paper into the filtering device and the device was then allowed to run for 15 minutes. After 15 minutes, the filter was weighed again to determine the particulate mass that had accumulated during this time period. This procedure was repeated with two more filters and the average of the three masses gave the TPM values for each chamber. The TPM values were adjusted to 30 $\mu g/m^3$, which resembles the values found in the homes of smokers by the EPA.
All cigarettes were smoked and stored in accordance with the Federal Trade Commission (FTC) smoking regimen. At the end of each week, cages were removed from the exposure chamber, bagged, and transported to the vivarium where mice were placed into the cages with the THS exposed material. For the next week, an identical set of cages and fabric was prepared and exposed to smoke in the same way as the first set of cages. By using two sets of cages and materials, each of which was exposed on alternating weeks, we ensured that mice inhabited cages containing fabric that had been exposed to fresh SHS in the beginning of each week and aged smoke towards the end week. Throughout the exposure period, hair was removed from the backs of the exposed mice (and controls) to mimic the bare skin of humans.

N-acetyl-p-aminophenol (APAP/tylenol) treatment: Four cohorts of male mice of the same age were used for *in vivo* APAP treatment studies. APAP was purchased from

Sigma (Cat# A5000-100G) and was dissolved in warm PBS and injected IP. THS-exposed mice and controls received a daily dose of 300 mg/kg for eight weeks via IP injections. The concentration of each APAP solution was adjusted so that all mice received approximately the same volume.

Antioxidant Therapy: Four cohorts of male mice, control and THS-exposed, were given antioxidants daily starting at weaning (3 weeks of age) for five months. We used N-acetylcysteine (NAC) and α-tocopherol (α –TOC). NAC (50 mg/kg) was dissolved in PBS and injected daily via IP. α-TOC (150 mg/kg) was dissolved in 70% ethanol and also injected IP daily.

Tissue Extracts: After six months of THS exposure, mice were sacrificed livers were extracted from THS-exposed or control mice, washed with PBS and immediately frozen. The frozen livers were stored at -80°C. Liver tissue was homogenized in radioimmunoprecipitation assay buffer (RIPA), centrifuged, and the supernatant collected unless otherwise specified by instruction manuals of the assay kits used in this study. Extracts were used to perform the various assays we used for this study.

Blood Extracts: Blood was extracted directly from the heart and allowed to coagulate on ice for 20-30 minutes. The samples were then centrifuged at 10,000 rpm for phase separation. The serum was used immediately for assays or frozen and stored at -80° C

and later used in assays.

Tissue embedding and Immunolabeling: Liver tissues from control and THS-exposed mice were fixed in 4% paraformaldehyde overnight, then rinsed in 1X PBS, incubated in 0.1 M glycine solution, followed by an incubation with 15% sucrose and subsequently 30% sucrose solution and embedded in optimal cutting temperature (O.C.T.) embedding medium (Cat# VWR 25608-930). Sections 8 μm thick were prepared and the tissue immunolabeled for 4-HNE, a marker for lipid peroxidation. Sections were blocked with 10% BSA, then incubated with mouse anti-HNE antibody (1:100) (Abcam; Cat # ab48506) overnight at 4°C, the excess primary Ab washed and the sections incubated with AlexaFluoro 568-labeled goat anti-mouse IgG antibody (1:3000) (Invitrogen; Cat# A-11004). The excess of secondary antibody was washed away, the sections mounted with Vectashield and imaged using a Nikon Microphot-FXA fluorescence microscope with a Nikon DS-Fi1 digital camera and Nikon NIS-Elements software (Nikon Instruments Inc., Melville, NY).

Measurement of SOD activity: Cayman Superoxide Dismutase Assay Kit (Cat # 706002) was used to measure SOD levels in the liver. Frozen liver pieces (10 mg) were placed in ice-cold RIPA buffer containing 50mM Tris (50mM pH 7), NaCl (150mM), SDS (0.1%), sodium deoxycholate (0.5%) and Triton X (1%) and homogenize using a Bullet Blender Homogenizer to extract total protein. The samples were centrifuged at 10,000 rpm for 15 min at 4°C, and the resulting supernatant was used for SOD activity

assay. Protein quantification was done using the Bradford assay (Bio-Rad). SOD activity was quantified by measuring the dismutation of superoxide radicals generated by xanthine oxidase and hypoxanthine. A standard curve was generated and used to quantify the activity of SOD in the liver samples.

Measurements of hydrogen peroxide levels: A Cayman Hydrogen Peroxide Assay Kit (Cat # 600050) was used to measure H_2O_2 levels in the liver. Fresh liver samples (10 mg) were homogenized in ice-cold RIPA buffer containing 50mM Tris (50mM pH 7), NaCl (150mM), SDS (0.1%), sodium deoxycholate (0.5%) and Triton X (1%) using a Bullet Blender Homogenizer to extract total protein. The samples were centrifuged at 10,000 rpm for 15 min at 4°C, and the resulting supernatant was collected for the assay. H_2O_2 was detected using 10-acetyl-3,7-dihydroxyphenoxazine (ADHP), a highly sensitive and stable probe for H_2O_2. In the presence of horseradish peroxidase, ADHP reacts with H_2O_2 in a 1:1 stoichiometry ratio to produce a highly fluorescent resorufin (excitation = 530-560 nm; emission = 590 nm). The standard curve generated was used to quantify the activity of hydrogen peroxide in the liver.

Measurement of catalase activity: Cayman Catalase Assay Kit was used to measure catalase (Cat # 707002) activity. Frozen liver pieces (10 mg) were placed in ice-cold RIPA buffer containing 50mM Tris (50mM pH 7), NaCl (150mM), SDS (0.1%), sodium deoxycholate (0.5%) and Triton X (1%) and homogenized using a Bullet Blender Homogenizer to extract total protein. The samples were centrifuged at 10,000 rpm for

15 minutes at 4°C, and the resulting supernatant was collected and used for the assay. 20µl of tissue homogenate were added to the wells of a 96 well plate along with 100µl of assay buffer and 30µl methanol and the reaction initiated by addition of 20µl H_2O_2. After incubation for 20mins, 30µl of potassium hydroxide was added to terminate the reaction. 30µl of 4-amino-3-hydrazino-5-mercapto-1,2,4-triazole (purpald), which is a chromogen, was added. After incubation for 10 minutes at RT, 10µl potassium periodate was added and incubated again at RT for five minutes. Absorbance was read at 540nm. The method is based on the reaction of the enzyme with methanol in the presence of an optimal concentration of H_2O_2. The formaldehyde produced was measured spectrophotometrically with 4- amino-3-hydrazino-5-mercapto-1,2,4-triazole (Purpald) as the chromogen. Purpald specifically forms a bicyclic heterocycle with aldehydes which, upon oxidation, changes from colorless to a purple color. The amount of catalase activity levels were calculated and standardized for protein using the Bradford method (Bio-Rad).

Measurements of GPx activity: Cayman GPx activity assay kit (Cat# 703102) was used to measure GPx (Cat # 703102) activity in the liver. Frozen liver pieces (10 mg) were homogenized in ice-cold RIPA buffer containing 50mM Tris (50mM pH 7), NaCl (150mM), SDS (0.1%), sodium deoxycholate (0.5%) and Triton X (1%) using a Bullet Blender Homogenizer to extract total protein. The samples were centrifuged at 10,000 rpm for 15 minutes at 4°C, and the resulting supernatant was collected and used for the assay. 20µl of liver homogenate were added to the wells of a 96 well plate along with 100µl of assay buffer and 50µl of co-substrate composed of NADPH, glutathione and

glutathione reductase. Reactions were initiated by addition of hydroperoxide, mixed for a few seconds, and absorbance was read at 340nm every minute to obtain at least 5 time points. The assay measured GPx activity indirectly by a coupled reaction with glutathione reductase (GR). Oxidized glutathione (GSSG), produced upon reduction of an organic hydroperoxide by GPx, was recycled to its reduced state by GR and NADPH. The oxidation of NADPH to NADP+ was accompanied by a decrease in absorbance at 340nm. The rate of decrease in the A340 was directly proportional to the GPx activity in the liver homogenate samples.

Measurement of DNA damage: DNA damage was measured using an ELISA Kit from Cell BioLabs Inc (Cat# STA-320) which allows the quantification of 8-hydroxy-2-deoxy Guanosine (8-OH-dG), DNA damage marker in ng/ml. DNA was extracted from liver samples, dissolved in water (1-5 mg/mL) and converted into single stranded DNA by incubating the sample at 95°C for five minutes following by chilling on ice. DNA was digested to nucleosides by incubating the denatured DNA with 5-20 units of nuclease P1 for 2 hours at 37°C at final concentration of 20 mM Sodium Acetate, pH 5.2, followed by treatment with 5-10 units of alkaline phosphatase for 1 hr at 37°C in a final concentration of 100 mM Tris, pH 7.5. The reaction mixture was centrifuged for five minutes at 6,000 rpm and the supernatant used for the 8- OH-dG ELISA assay. 50 µL of experimental samples or 8-OHdG standards were added to the wells of the 8-OHdG Conjugate coated plate. Incubation was performed at room temperature for 10min on an orbital shaker. 50 µL of anti-8-OHdG antibody was added to each well and the plate was incubated at room

temperature for 1hr. The microwells were then washed three times with Wash Buffer. After the last wash, 100 μL of secondary Antibody-Enzyme Conjugated was added and incubation was performed at room temperature for 1 hr followed by three washes. 100 ul of Substrate Solution containing 3,3', 5,5'Tetramethylbenzidine was added to each well and incubated at room temperature for 30 minutes. The enzyme reaction was stopped by addition of 100 μL of Stop Solution into each well. Absorbance was read on a spectrophotometer at λ=450 nm.

Measurement of nitrosylation of proteins: Protein damage was quantified by measuring the nitrosylation of tyrosine residues in proteins. The amount of 3-nitrotyrosine in the liver proteins was determined using the OxiSelect Nitrotyrosine ELISA Kit from Cell Biolabs (Cat# STA-305). The liver samples or nitrated BSA standards were first added to a nitrated BSA pre-absorbed enzyme immunoassay (EIA) plate. After a brief incubation, an anti-nitrotyrosine antibody was added, followed by an HRP conjugated secondary antibody. The protein nitrotyrosine content in the liver samples were determined by comparing with a standard curve that was prepared from predetermined nitrated BSA standards provide in the kit.

Measurement of lipid peroxidation: Lipid peroxidation in the liver was determined by the levels of the byproduct of lipid peroxidation known as malaldehyde (MDA) using the OxiSelect TBARS Assay Kit from Cell Biolabs (Cat # STA-330). The unknown MDA containing samples or MDA standards were first reacted with Thiobarbituric Acid (TBA)

at 95°C for 60 minutes. After this incubation period, the plate containing the samples and standards was read fluorometrically at 540 nm excitation and 590 nm emission. The MDA content in unknown samples was determined by comparison with the predetermined MDA standard curve.

Measurement of AST levels: The AST levels were measured using the Aspartate aminotransferase (AST) Activity Assay (Cat# MAK055). 100 uL of the reaction mix (80 uL AST Assay buffer; 2 uL AST enzyme mix; 8 uL AST developer; 10 uL AST substrate) was added to each well. The plate was then mixed by pipetting and incubated at 37^{O}C and was protected from light. The first initial reading was taken after 2 minutes of incubation. After the recording of the first initial reading, the subsequent readings where taken every five minutes until the measurements of the samples where greater than the value of the highest standard (~10nmole/well). The background in the wells was corrected by subtracting the final reading of standard zero from all the final readings of the eight standards. The standards were then used to make a standard curve. The AST activity was calculated by subtracting the final reading of each sample from initial reading divided by the reaction rate and volume of the sample.

Measurement of ATP levels: The ATP levels in liver were quantified using BioVision's ATP Colorimetric and Fluorometric Assay kit (Cat# K354-100), which is designed to detect low quantities of ATP (~50pmol) by measuring the phosphorylation of glycerol. The assay was performed according to the protocol included in the kit. Liver

tissue samples (10mg) were homogenized in 100 µl of ATP assay buffer and 50 µl of sample supernatant was added to a 96-well plate in duplicates. 50 µl of the Reaction Mix (44 µl ATP Assay buffer; 2µl ATP probe; 2 µl ATP converter; and 2 µl developer) was added to each well containing the ATP standards and samples to initiate the phosphorylation of glycerol reaction. The plate was mixed well and incubated for 30 minutes at room temperature away from light. During this incubation period, glycerol was phosphorylated. The product of this phosphorylation reaction was read at λ=570nm and the absorbance readings of the standards were used to generate a standard curve. The unknown amount of ATP in the samples was then calculated using the standard curve and the observances reading of the samples.

Measurement of Urea levels: Urea levels in the liver tissue were quantified using Cell Biolabs' Urea Assay Kit (Cat # sta-382), which is based on the Berthelot reaction. The enzyme urease is used to catalyze the hydrolysis of urea into carbon dioxide and ammonia. Ammonia then reacts with the alkaline developer (Berthelot's reagent) included in this kit to produce a blue-green colored product that can be measured with a standard spectrophotometric plate reader at an optical density 630nm. 10 µl of the standards or samples were added to the 96-well plate. 100 µl of the urease/Ammonia Reagent (40 mg of urease for 10 mL of Ammonia reagent) mixture was added to each well. The plate was mixed and incubated for 10 minutes at 37^{o}C. After incubation, 100 µl of the Developing Reagent was added to each well using a multichannel pipette. The

plate was placed on an orbital shaker to mix the samples and then incubated 30 minutes at 37^{O}C. After incubation period the plate was read at 630 nm.

Measurement of Sirtuin 1 levels: SIRT1 levels were quantified using SIRT1 Sandwich Enzyme Immunoassay from Mybiosource (Cat # MBS2023445). This kit includes a 96-well strip plate pre-coated with an antibody specific to SIRT1. 100 µl of standards or samples were added to the plate wells with a biotin-conjugated antibody specific to SIRT1 and incubated for 2 hours at 37 °C.100 µl of Detection Reagent A working solution was added to each well and the plate covered and incubated for 1 hour at 37^{O}C. After the incubation period the plate was washed three times with 350 µl of wash solution for each well usingmulti-channel pipette. The plate was allowed to sit for 2 minutes and excess liquid was removed by pressing the plate onto absorbent paper towels. 100 µl of Detection Reagent B working solution was then added to each well and the covered plate was incubated for 30 minutes at 37^{O}C. The plate was then washed with 350 µl of wash solution five times. 90 µl of Tetramethylbenzidine (TMB) Substrate Solution was then added to each well (samples turned blue) and the covered well plate was incubated for 15 minutes at 37^{O}C. The plate was protected from light. 50µL of Stop Solution was added to each well to stop the reaction and the plate was placed on a shaker to mix the samples well. A microplate reader was used to measure the OD readings of the standards and samples at 450nm.

Measurement of AMPK-P levels: The AMPK-P levels in the samples were quantified using an AMPKα pT172 ELISA Kit (Cat # ab154468). This kit contains a 96 well plate which is pre-coated with a specific mouse monoclonal antibody specific for AMPKα pT172. 25 µl of standards (Hek293T cells) or samples were added to the wells along with the rabbit monoclonal primary detector antibody and the plate was incubated for three hours at room temperature. The plate was then washed with 300 µl of 1X wash buffer to eliminate any unbound standard or samples in the plate. After washing and drying of the plate, 50 µl of horseradish peroxidase (HRP)- conjugated secondary detector antibody (HRP Label) specific for the primary detector antibody was added to wells. After incubation, the well plate was washed again three times using 300 µl of 1X wash buffer. Then 100 µl of a Tetramethylbenzidine (TMB) substrate solution was added to the wells and the wells changed in color depending on the amount of AMPKα pT172 bound present in the samples. The OD of the samples was then measured at 600 nm and used to calculate the amount of each AMPK-P in each sample. A standard curve was created and the unknown samples were extrapolated this standard curve.

Statistical Analysis: For the statistical analysis of experiments, we used Graphpad Instat Software (Graphpad, La Jolla, CA, USA). Statistical comparisons between two-groups was performed using the unpaired Student's *t*-test. All data are mean±SD represented by the error bars. Means were considered significantly different when $p<0.05$.

Results

THS exposure leads to increased oxidative stress in the liver

Previously, we showed that 30 % of the mice exposed to THS toxins develop a fatty liver [32]. We hypothesize that exposure to THS toxins leads to lipid accumulation in the liver of THS-exposed mice by increasing oxidative stress. Under normal conditions, the hepatocytes balance oxidative stress with the help of two important antioxidant enzymes, catalase and glutathione peroxidase (GPx). These enzymes regulate the levels of hydrogen peroxide (H_2O_2) in the liver. Catalase converts H_2O_2 into water and oxygen whereas GPx converts it into water only **(**Figure 2.1A). THS-exposed mice have higher superoxide dismutase (SOD) activity and as a result they also have higher levels of H_2O_2 in the liver than do the controls (Figure 2.1B-C). Because there is no significant increase in catalase or GPx activity, H_2O_2 is not properly been processed and the levels of reactive oxygen species (ROS) remain high in the liver (Figure 2.1 D-E). To further support these results, we measured the $NADP^+$/NADPH ratio, which is an indicator of the cell reducing potential, because GPx activity is coupled to the reduction of NADPH to $NADP^+$. The $NADP^+$/NADPH ratio is significantly lower in THS-exposed mice than in control mouse livers (Figure 2.1F), showing that the reduction potential of these animals is decreased and might result in their inability to reduce the oxidative stress levels induced by the THS toxins.

THS-induced ROS lead to molecular and cellular damage in the liver

High levels of H_2O_2 in cells can lead to the production of hydroxyl radicals via the Fenton reaction in the presence of ferrous iron ion (Fe^{2+}) (Figure 2.2A). These radicals can damage lipids and proteins, and lead to the formation of DNA adducts. We found that in the liver of THS-exposed mice there are significantly higher levels of lipid peroxidation, protein nitrosylation and DNA damage (Figure 2.2B-D and 2.S1). We also investigated whether THS toxins result in functional damage in the liver by measuring ATP, aspartate aminotransferase (AST) and urea levels. ATP is a marker for mitochondria function whereas AST and urea are markers of liver health. THS-exposed mice produced lower ATP levels than the controls (Figure 2.2E), suggesting that the ability of the mitochondria in THS-exposed mice to synthesize cellular energy is decreased. High levels of AST suggest liver damage whereas high levels of urea suggesting increase in amino acid metabolism (Figure 2.2F,G). Together, these results show that THS toxins result in damage of liver function.

Oxidative stress mediated damage is improved by treating the mice with antioxidants

To investigate whether the THS-induced oxidative stress in the liver can be reversed, we treated the THS-exposed mice with the antioxidants N-acetylcysteine (NAC) and α-tocopherol (α –TOC) for five months. These two antioxidants have been used previously to treat oxidative stress in different tissues [46-48]. Treatment with these antioxidants for five months while the mice were being exposed to THS, leads to a decrease in oxidative stress. These mice have SOD activity and H_2O_2 levels similar to

those of the non-exposed mice treated with antioxidants but significantly lower than THS-exposed mice without treatment with antioxidants (Figure 2.3A,B). Although no significant changes were observed in the activity of catalase (Figure 2.3C), the THS-exposed mice treated with antioxidants have higher GPx activity than THS-exposed non-treated mice (Figure 2.3D). The same occurred for the $NADP^+$/NADPH ratio (Figure 2.3E). Furthermore, NAC and α-TOC lowered the total hepatic lipid weight in the THS-exposed mice (Figure 2.3F).

Treatment with antioxidant agents also decreased the oxidative-stress-mediated molecular damage in THS-exposed mice. These mice have lower lipid peroxidation (Figure 2.4A) and lower protein damage (Figure 2.4B) in THS exposed mice. However, no significant improvement was observed in DNA damage (Figure 2.4C). We also investigated whether antioxidant treatment improved functional damage by measuring ATP, AST and urea. AST is responsible for the conversion of aspartate to α-ketoglutarate to oxaloacetate and glutamate, which is fundamental for the function of the liver. Urea is a by-product of amino acid metabolism that occurs in the liver. Antioxidant treatment did not improve these parameters (Figure 2.4D-F).

Treatment of THS-exposed mice with APAP increases oxidative-stress-mediated damage

Because N-acetyl-p-aminophenol (APAP/Tylenol) is a common drug taken by many people, especially by children, and it is known to damage the liver if taken in high doses [49], we investigated whether giving THS-exposed mice Tylenol would further increase

oxidative stress in the liver. We used a dose the APAP/Tylenol that has been previously shown to induce chemical damage in the liver without killing the animals [49-51]. Based on these studies, we treated the THS-exposed mice for eight weeks with APAP/Tylenol. THS-exposed mice treated with APAP/Tylenol have higher SOD activity and higher H_2O_2 levels than THS-exposed non-treated mice (Figure 2.5A and B). Moreover, the levels of catalase activity were significantly decreased when compare with THS exposed non-APAP treated animals (Figure 2.5 C). We also observed that although GPx activity was not changed (Figure 2.5D), the $NADP^+$/NADPH ratio was significantly decreased (Figure 2.5E), showing that the reducing potential in the THS-exposed APAP-treated mice was low. Furthermore, APAP/Tylenol increased the total hepatic lipid weight in the THS-exposed mice (Figure 2.5F). This, results in further damage to the ability of the liver to handle the oxidative stress damage induced by THS.

We also quantified the oxidative stress-induced molecular damage and observed that THS exposure in conjunction with APAP/Tylenol treatment results in much higher levels of lipid peroxidation (Figure 2.6A), higher protein nitrosylation (Figure 2.6B) and higher DNA damage (Figure 2.6C). In addition, we also measured the ATP, AST and urea levels. High levels of AST and urea are associated with abnormal liver function [52-53]. APAP treatment results in lower ATP levels in THS-exposed mice suggesting that these mice have dysfunctional mitochondria (Figure 2.6D). APAP/Tylenol treatment results in higher AST levels in these animals suggesting that when THS exposure and APAP/Tylenol treatment are combined, further functional damage to the liver occurs (Figure 2.6E). However, APAP/Tylenol treatment of the THS-exposed mice did not have

increased urea levels when compared to exposure only to THS (Figure 2.6F).

THS toxins inhibit the SIRT1/AMPK/ SBREP1c signaling pathway in the liver.

To investigate the cellular and molecular mechanisms of THS-induced lipid metabolism, we performed genomic analysis using both DNA microarray and RNA-Seq and found that Sirtuin 1 (SIRT1), a key regulator of lipid metabolism, is down regulated in THS-exposed mice. SIRT1 modulates the activity of other metabolic energy regulators such as 5' AMP-activated protein kinase (AMPK). AMPK is an energy sensor within the cell that responds to energy depletion (decrease in ATP production) or any other cellular damage insult that result in alterations to cellular energy. Together, SIRT1 and AMPK regulate lipid metabolism by preventing the synthesis of lipids and by stimulating fatty acid oxidation [54-68]. It has been shown using SIRT1 transgenic mice showed SIRT1 is required for activation of that AMPK and improvement of mitochondrial function [67]. It has also been shown AMPK phosphorylates and inhibits SREBP1c in diet induced insulin resistant mice [68]. Taken together studies suggest that SIRT1 and AMPK both work to prevent abnormal lipid metabolism by targeting and inhibiting SREBP1c a key lipigenic enzyme in the liver. Therefore, we investigated the SIRT1/AMPK/SREBP1c pathway and whether the THS-induced hepatic steatosis is a result of alterations in this pathway. When compared to the control mice the THS-exposed animals have lower levels of SIRT1 and of phosphorylated AMPK, the active form of this enzyme (Figure 2.7A,B). Because activated AMPK is decreased in THS-exposed mice we tested the levels of SREBP1c the levels of SREBP1c. We found that in THS-exposed mice

SREBP1c is elevated, leading to higher levels of lipids in the liver (Figure 2.7C). These findings suggest that THS exposure stimulate hepatic steatosis by altering the SIRT1/AMPK/SREBP1c pathway.

Discussion

We have previously shown that THS exposure results in oxidative stress mediated damage of multiple organs in mice including steatosis of the liver [32]. Here we show that the lipid accumulation is correlated with increase in the levels of oxidative stress, primarily of ROS, and inhibition of the SIRT1/AMPK/SREBP1c pathway (Figure 8A). Modulating the levels of ROS with antioxidants resulted in reduction of the THS-induced hepatic steatosis whereas treatment with APAP resulted in augmentation of the THS-induced the lipid accumulation (Figure 8B).

We showed that, in the THS-exposed mice, the oxidative stress did not result in organ failure nor did the mice die. Data from a cytokine array performed on the serum of these mice showed that there is a small increase in pro-inflammatory cytokines and chemokines, indicating that THS-exposed mice have very low levels of inflammation [32] but we do not think that the low levels of inflammation have an effect on development of steatosis. For example, TNF-α and IL-1β, cytokines that have been associated with hepatic steatosis, were not altered in the THS-exposed mice [69-71]. However, we did see significant changes in SIRT1, AMPK and SREBP1c, which are known to be critically involved in lipid metabolism. Therefore, we focused our studies on the SIRT1/AMPK/SREPB1c pathway to determine if oxidative stress altered this pathway and resulted in THS-induced hepatic steatosis.

The oxidative stress mediated damage to the hepatic lipids, proteins, and DNA have a detrimental effect for lipid metabolism [72-74]. The liver is one of the major metabolic organs where glucose is metabolized, modified and stored. Perturbations in the

metabolism and storage of glucose as well as insulin resistance in the liver have been linked to the development of hepatic steatosis [74-76]. It is known that lipid peroxidation results in a decrease in the uptake of glucose in cortical rat neurons, which in the short term leads to abnormal glucose metabolism but over time it may lead to cell death [77]. Lipid peroxidation can also lead to conformational changes in the lipid bilayer and these changes can potentially alter the localization and stability of many receptors involved in lipid metabolism [78].

THS-exposed mice have high levels of protein damage, which affect the expression, and levels of proteins involved in the regulation of lipid metabolism in the liver. SIRT1 is a key regulator of lipid metabolism and it is known to work together with AMPK to prevent lipid accumulation in the liver by inhibiting SREBP1c and increasing fatty acid metabolism [54-68]. In this study we show that THS toxins alter the SIRT1/AMPK/SREBP1c signaling axis by decreasing SIRT1 levels which lead to decrease in phosphorylated/activated AMPK resulting in increase of SREBP1c and increase in lipid synthesis, with subsequent development of hepatic steatosis (Figure 8A). We also show that the liver specific damage we observed in the THS-exposed mice is mediated by oxidative stress triggered by the THS toxins. Increasing the oxidative stress in the liver of THS-exposed mice with APAP/Tylenol worsened lipid accumulation whereas when the mice were exposed to THS and treated with antioxidants there was a decrease in lipid accumulation.

APAP/Tylenol is commonly used to treat headaches and fever and when taken for prolonged periods of time or higher dose it is known to cause liver damage. This can

occur by depletion of glutathione (GSH) and by increasing mitochondria damage [79-81]. When we treated THS-exposed mice with APAP, we observed that these mice have higher liver damage than mice only exposed to THS. These mice also have lower levels of ATP, which suggest impaired mitochondria function. AST levels were also elevated suggesting abnormality in amino acid metabolism in the liver.

To decrease oxidative stress we treated THS-exposed mice with NAC and α-TOC, which have been commonly used in humans and rodents for that purpose [82-84]. NAC is derivative of the amino acid L-cysteine and it is a direct precursor of glutathione consequently it has direct and indirect antioxidant properties [83]. Its free thiol group can interact with the electrophilic groups found in reactive oxygen species (ROS) agents. NAC can behave as an indirect antioxidant in the glutathione synthesis pathway, an antioxidant enzyme that decreases cellular oxidative stress [83]. α-TOC is an important lipid-soluble antioxidant that reacts with lipid radicals and consequently less lipid peroxidation occurs preventing damage to the plasma and mitochondrial membranes [84].

In conclusion, these studies provide insight into the effects of THS toxins on key molecules in lipid metabolism such as the SIRT1/AMPK/SIRT1 signaling pathway. We show that by altering the oxidative stress levels using APAP/tylenol or the antioxidant agents NAC and α-TOC, we alter the THS-induced damage, which indicates that the THS-induced damage is mediated by oxidative stress. Based on our results, it is clear that THS toxins have the ability to alter fundamental metabolic processes such as lipid metabolism resulting in steatosis making THS a new risk factor for hepatic steatosis.

References

1. Thus, T. H. S. (2016). Third hand smoke–A hidden demon. Oral oncology 54: e3-e4.

2. U.S. Department of Health and Human Services. The Health Consequences of Involuntary Exposure to Tobacco Smoke: A Report of the Surgeon General. 2006. Available:http://www.surgeongeneral.gov/library/secondhandsmoke/report/index.html [accessed 24 August 2014]

3. Foronjy, R. F, Mirochnitchenko, O, Propokenko, O, Lemaitre, V, Jia, Y, (2006). Superoxide dismutase expression attenuates cigarette smoke–or elastase-generated emphysema in mice. American journal of respiratory and critical care medicine, 173(6), 623-631.

4. Visioli F, Galli C, Plasmati E, Viappiani S, Hernandez A, (2000). Olive phenol hydroxytyrosol prevents passive smoking–induced oxidative stress. Circulation, 102(18), 2169-2171.

5. Zalata A, Yahia S, El-Bakary A, Elsheikha H. M. (2007). Increased DNA damage in children caused by passive smoking as assessed by comet assay and oxidative stress. Mutation Research/Genetic Toxicology and Environmental Mutagenesis, 629(2), 140-147.

6. Kosecik M, Erel O, Sevinc E, Selek, S. (2005). Increased oxidative stress in children exposed to passive smoking. International journal of cardiology, 100(1), 61-64.
7. Aycicek A, Erel O, Kocyigit A. (2005). Increased oxidative stress in infants exposed to passive smoking. European journal of pediatrics, 164(12), 775-77.

8. Bermudez E, Stone K, Carter KM, Pryor WA (1994). Environmental tobacco smoke is just as damaging to DNA as mainstream smoke. Environ. Health Perspect 102, 870–874

9. Knight-Lozano CA, Young CG, Burow DL, Hu, ZY, Uyeminami D, (2002). Cigarette smoke exposure and hypercholesterolemia increase mitochondrial damage in cardiovascular tissues. Circulation, 105(7), 849-854.
10. Winickoff JP, Friebely J, Tanski SE, Sherrod C, Matt GE, et al. (2009) Beliefs about the health effects of "thirdhand" smoke and home smoking bans. Pediatrics 123: e74-e79.
11. Burton A (2011) Does the smoke ever really clear? Thirdhand smoke exposure raises new concerns. Environ Health Perspective 119: A70-74.

12. Whitehead T, Metayer C, Ward MH, Nishioka MG, Gunier R, et al (2009). Is house-dust nicotine a good surrogate for household smoking?. American journal of epidemiology 169: 1113-1123.

13. Sleiman M, Gundel LA, Pankow JF, Jacob P, Singer, BC, et al. (2010) Formation of carcinogens indoors by surface-mediated reactions of nicotine with nitrous acid, leading to potential thirdhand smoke hazards. Proceedings of the National Academy of Sciences 107: 6576-6581.

14. Van Loy MD, Riley WJ, Daisey JM, Nazaroff WW (2001) Dynamic behavior of semivolatile organic compounds in indoor air. 2. Nicotine and phenanthrene with carpet and wallboard. Environmental Science & Technology 35: 560-567.

15. Caldwell WS, Greene JM, Plowchalk DR, DeBethizy JD (1991) The nitrosation of nicotine: a kinetic study. Chemical research in toxicology 4: 513-516.

16. Singer BC, Revzan KL, Hotchi T, Hodgson AT, Brown NJ (2004) Sorption of organic gases in a furnished room. Atmospheric Environment 38: 2483-2494.

17. Sleiman M, Destaillats H, Smith JD, Liu CL, Ahmed M (2010) Secondary organic aerosol formation from ozone-initiated reactions with nicotine and secondhand tobacco smoke. Atmospheric Environment 44: 4191-4198.

18. Hoffmann D, Brunnemann KD, Prokopczyk B, Djordjevic MV (1994) Tobacco-specific N-nitrosamines and ARECA-derived N-nitrosamines: Chemistry, biochemistry, carcinogenicity, and relevance to humans. Journal of Toxicology and Environmental Health, Part A Current Issues 41: 1-52.

19. Hecht SS (1998) Biochemistry, biology, and carcinogenicity of tobacco-specific N-nitrosamines. Chemical research in toxicology 11: 559-603.

20. Matt GE, Quintana PJE, Hovell MF, Bernert JT, Song S, Novianti N, (2004) Households contaminated by environmental tobacco smoke: sources of infant exposures. Tobacco control 13: 29-37.

21. Centers for Disease Control and Prevention (2011) Smoking and Tobacco Use: Data and Statistics.http://www.cdc.gov/tobacco/data_statistics.

22. Hecht SS, Carmella SG, Le KA, Murphy SE, Boettcher AJ, et al. (2006) 4-(methylnitrosamino)-1-(3-pyridyl)-1-butanol and its glucuronides in the urine of infants exposed to environmental tobacco smoke. Cancer Epidemiology Biomarkers & Prevention 15: 988-992.

23. Singh GK, Siahpush M, Kogan MD (2010) Disparities in children's exposure to environmental tobacco smoke in the United States, 2007. Pediatrics 10.1542/peds: 2009-2744.

24. Thomas JL, Guo H, Carmella SG, Balbo S, Han S, et al. (2011) Metabolites of a tobacco-specific lung carcinogen in children exposed to secondhand or thirdhand tobacco smoke in their homes. Cancer Epidemiology Biomarkers & Prevention 20: 1213-1221.

25. Hang B, Sarker AH, Havel C, Saha S, Hazra TK , et al. (2013) Thirdhand smoke causes DNA damage in human cells. Mutagenesis 28: 381-391.

26. Roberts JW, Dickey P (1995). Exposure of children to pollutants in house dust and indoor air. In Reviews of environmental contamination and toxicology 143: 59-78.

27. Xu B, Chen M, Yao M, Ji X, Mao Z, et al. (2015) Metabolomics reveals metabolic changes in male reproductive cells exposed to thirdhand smoke. Scientific reports 6.

28. Rehan VK, Sakurai R, Torday JS (2011) Thirdhand smoke: a new dimension to the effects of cigarette smoke on the developing lung. American Journal of Physiology-Lung Cellular and Molecular Physiology 301: L1-L8.

29. Yolton K, Dietrich K, Auinger P, Lanphear BP, Hornung R (2005) Exposure to environmental tobacco smoke and cognitive abilities among US children and adolescents. Environmental health perspectives 2005:98-103.

30. Elliot J, Vullermin P, Robinson P (1998) Maternal cigarette smoking is associated with increased inner airway wall thickness in children who die from sudden infant death syndrome. American Journal of respiratory and critical care medicine 158: 802-806.

31. Jung JW, Ju YS, Kang HR (2012) Association between parental smoking behavior and children's respiratory morbidity: 5-year study in an urban city of South Korea. Pediatric pulmonology 47: 338-345.

32. Martins-Green M, Adhami N, Frankos M, Valdez M, Goodwin B, et al. (2014) Cigarette smoke toxins deposited on surfaces: implications for human health. PloS one 9: E86391.

33. Adhami N, Starck SR, Flores C, Green MM (2016) A Health Threat to Bystanders Living in the Homes of Smokers: How Smoke Toxins Deposited on Surfaces Can Cause Insulin Resistance. PloS one 11: e0149510.

34. Erickson SK (2009) Nonalcoholic fatty liver disease. Journal of lipid research 50: S412-S416.

35. Marrero JA, Fontana RJ, Su GL, Conjeevaram HS, Emick DM, et al. (2002) NAFLD may be a common underlying liver disease in patients with hepatocellular carcinoma in the United States. Hepatology 36: 1349-1354.

36. Cazanave SC, Sanyal AJ (2016) Molecular Mechanisms of Lipotoxicity in Nonalcoholic Fatty Liver Disease. In Hepatic De Novo Lipogenesis and Regulation of Metabolism. Springer International Publishing.

37. Tiniakos DG, Vos MB, Brunt EM (2010) Nonalcoholic fatty liver disease: pathology and pathogenesis. Annual Review of Pathological Mechanical Disease 5: 145-171.

38. Lettéron P, Sutton A, Mansouri A, Fromenty B, Pessayre D (2003) Inhibition of microsomal triglyceride transfer protein: Another mechanism for drug-induced steatosis in mice. Hepatology 38: 133-140.

39. Fromenty B, Pessayre D. (1997) Impaired mitochondrial function in microvesicular steatosis effects of drugs, ethanol, hormones and cytokines. Journal of hepatology 26: 43-53.

40. Azzalini L, Ferrer E, Ramalho LN, Moreno M, Domínguez M, et al. (2010) Cigarette smoking exacerbates nonalcoholic fatty liver disease in obese rats. Hepatology 51: 1567-1576.

41. Browning JD, Horton JD (2004) Molecular mediators of hepatic steatosis and liver injury. The Journal of clinical investigation 114: 147-152.

42. Tolosa L, Gómez-Lechón MJ, Jiménez N, Hervás D, Jover R, et al. (2016) Advantageous use of HepaRG cells for the screening and mechanistic study of drug-induced steatosis. Toxicology and Applied Pharmacology.

43. Petersen KF, Dufour S, Befroy D, Lehrke M, Hendler RE, et al. (2005) Reversal of nonalcoholic hepatic steatosis, hepatic insulin resistance, and hyperglycemia by moderate weight reduction in patients with type 2 diabetes. Diabetes 54: 603-608.

44. Ryan MC, Itsiopoulos C, Thodis T, Ward G, Trost N, et al. (2013) The Mediterranean diet improves hepatic steatosis and insulin sensitivity in individuals with non-alcoholic fatty liver disease. Journal of hepatology 59: 138-143.

45. Faghihzadeh F, Adibi P, Rafiei R, Hekmatdoost A (2014) Resveratrol supplementation improves inflammatory biomarkers in patients with nonalcoholic fatty liver disease. Nutrition research 34: 837-843.

46. de Diego-Otero Y, Romero-Zerbo Y, el Bekay R, Decara J, Sanchez L, Rodriguez-de Fonseca F (2009) α-tocopherol protects against oxidative stress in the fragile X knockout mouse: an experimental therapeutic approach for the Fmr1 deficiency. Neuropsychopharmacology 34: 1011-1026.

47. Thakurta IG, Banerjee P, Bagh MB, Ghosh A, Sahoo A, et al. (2014) Combination of N-acetylcysteine, α-lipoic acid and α-tocopherol substantially prevents the brain synaptosomal alterations and memory and learning deficits of aged rats. Experimental gerontology 50: 19-25.

48. Joseph, AJ, Adamu, KB, Shu'aibu Yahya BRL, Martina BS, Asabe MUA, et al. (2014) Influence of high dietary vitamin C and E oral administration on anemia and organ damage in wistar rat infected with Trypanosoma brucei brucei (Federe strain).

49. Jaw S, Jeffery EH (1993) Interaction of caffeine with acetaminophen: 1. Correlation of the effect of caffeine on acetaminophen hepatotoxicity and acetaminophen bioactivation following treatment of mice with various cytochrome P450 inducing agents. Biochemical pharmacology 46: 493-501.

50. Zaher H, Buters JT, Ward JM, Bruno, MK, Lucas AM, et al. (1998) Protection against acetaminophen toxicity in CYP1A2 and CYP2E1 double-null mice. Toxicology and applied pharmacology 152: 193-199.

51. Shayiq RM, Roberts DW, Rothstein K, Snawder J E, Benson W, et al. (1999) Repeat exposure to incremental doses of acetaminophen provides protection against acetaminophen-induced lethality in mice: An explanation for high acetaminophen dosage in humans without hepatic injury. Hepatology 29: 451-463.

52. Abdel-Daim MM, Abuzead, SM, Halawa SM (2013) Protective role of Spirulina platensis against acute deltamethrin-induced toxicity in rats. PLoS One 8: e72991.

53. Puche JE, Lee YA, Jiao J, Aloman C, Fiel MI, et al. (2013) A novel murine model to deplete hepatic stellate cells uncovers their role in amplifying liver damage in mice. Hepatology 57: 339-350.

54. Caito S, Rajendrasozhan S, Cook S, Chung S, Yao H, et al. (2010) SIRT1 is a redox-sensitive deacetylase that is post-translationally modified by oxidants and carbonyl stress. FASEB Journal 24: 3145–3159.

55. Merksamer PI, Liu Y, He W, Hirschey MD, Chen D, et al (2013) The sirtuins, oxidative stress and aging: an emerging link. Aging 5: 144-150.

56. Purushotham A, Schug TT, Xu Q, Surapureddi S, Guo X, et al (2009) Hepatocyte-specific deletion of SIRT1 alters fatty acid metabolism and results in hepatic steatosis and inflammation. Cell metabolism 9: 327-338.

57. Brunet A, Sweeney LB, Sturgill JF, Chua, KF, Greer PL, et al (2004) Stress-dependent regulation of FOXO transcription factors by the SIRT1 deacetylase. Science 303: 2011-2015.

58. Webster BR, Lu Z, Sack MN, Scott I (2012) The role of sirtuins in modulating redox stressors. Free radical biology and medicine 52: 281-290.

59. Chen WL, Kang CH, Wang SG, Lee HM (2012) α-Lipoic acid regulates lipid metabolism through induction of sirtuin 1 (SIRT1) and activation of AMP-activated protein kinase. Diabetologia 55: 1824-1835.

60. Walker AK, Yang F, Jiang K, Ji JY, Watts JL, et al. (2010) Conserved role of SIRT1 orthologs in fasting-dependent inhibition of the lipid/cholesterol regulator SREBP. Genes & development 24: 1403-1417.

61. Rodgers JT, Puigserver P (2007) Fasting-dependent glucose and lipid metabolic response through hepatic sirtuin 1. Proceedings of the National Academy of Sciences 104: 12861-12866.

62. Ponugoti B, Kim DH, Xiao Z, Smith Z, Miao J, et al. (2010) SIRT1 deacetylates and inhibits SREBP-1C activity in regulation of hepatic lipid metabolism. Journal of Biological Chemistry 285: 33959-33970.

63. Kim E, Choi Y, Jang J, Park T (2013) Carvacrol protects against hepatic steatosis in mice fed a high-fat diet by enhancing SIRT1-AMPK signaling. Evidence-Based Complementary and Alternative Medicine 2013: 290104.

64. Yuan H, Shyy JYJ, Martins-Green M (2009) Second-hand smoke stimulates lipid accumulation in the liver by modulating AMPK and SREBP-1. Journal of hepatology 51: 535-547.

65. Jung EJ, Kwon SW, Jung BH, Oh SH, Lee BH (2011) Role of the AMPK/SREBP-1 pathway in the development of orotic acid-induced fatty liver. Journal of lipid research 52: 1617-1625.

66. Ahmed MH, Byrne CD (2007) Modulation of sterol regulatory element binding proteins (SREBPs) as potential treatments for non-alcoholic fatty liver disease (NAFLD). Drug discovery today 12: 740-747.

67. Price NL, Gomes AP, Ling AJ, Duarte FV, Martin-Montalvo A, et al. (2012) SIRT1 is required for AMPK activation and the beneficial effects of resveratrol on mitochondrial function. Cell metabolism 15: 675-690.

68. Li Y, Xu S, Mihaylova MM, Zheng B, Hou X, et al. (2011) AMPK phosphorylates and inhibits SREBP activity to attenuate hepatic steatosis and atherosclerosis in diet-induced insulin-resistant mice. Cell metabolism 13: 376-388.

69. Yin M, Wheeler MD, Kono H, Bradford BU, Gallucci RM, et al. (1999) Essential role of tumor necrosis factor alpha in alcohol-induced liver injury in mice. Gastroenterology 117:942-952.

70. Miura K, Kodama Y, Inokuchi S, Schnabl B, Aoyama T, et al. (2012) Toll-like receptor 9 promotes steatohepatitis by induction of interleukin-1beta in mice. Gastroenterology 2010;139:323-34.e7.

71. Lawler JF Jr, Yin M, Diehl AM, Roberts E, Chatterjee S. (1998) Tumor necrosis factor-alpha stimulates the maturation of sterol regulatory element binding protein-1 in human hepatocytes through the action of neutral sphingomyelinase. J Biol Chem 273:5053-5059.

72. Seki S, Kitada T, Yamada T, Sakaguchi H, Nakatani K, et al. (2002) In situ detection of lipid peroxidation and oxidative DNA damage in non-alcoholic fatty liver diseases. Journal of hepatology 37: 56-62.

73. Pan M, Cederbaum AI, Zhang YL, Ginsberg HN, Williams KJ, et al. (2004) Lipid peroxidation and oxidant stress regulate hepatic apolipoprotein B degradation and VLDL production. The Journal of clinical investigation 113: 1277-87.

74. Bryant RJ, Ryder J, Martino P, Kim J, Craig BW (2003) Effects of vitamin E and C supplementation either alone or in combination on exercise-induced lipid peroxidation in trained cyclists. The Journal of Strength & Conditioning Research 17: 792-800.

75. Flannery C, Dufour S, Rabøl R, Shulman GI, Petersen KF (2012) Skeletal muscle insulin resistance promotes increased hepatic de novo lipogenesis, hyperlipidemia, and hepatic steatosis in the elderly. Diabetes 61: 2711-2717.

76. Perry R J, Samuel VT, Petersen KF, Shulman GI (2014) The role of hepatic lipids in hepatic insulin resistance and type 2 diabetes. Nature 510: 84-91.

77. Lovell MA, Xie C, Markesbery WR (2000) Acrolein, a product of lipid peroxidation, inhibits glucose and glutamate uptake in primary neuronal cultures. Free Radical Biology and Medicine 29: 714-720.

78. Catalá A (2012) Lipid peroxidation modifies the picture of membranes from the "Fluid Mosaic Model" to the "Lipid Whisker Model". Biochimie 94: 101-109.

79. Reid, AB, Kurten RC, McCullough SS, Brock RW, Hinson JA (2005) Mechanisms of acetaminophen-induced hepatotoxicity: role of oxidative stress and mitochondrial permeability transition in freshly isolated mouse hepatocytes. Journal of Pharmacology and Experimental Therapeutics 312: 509-516.

80. Xie Y, McGill MR, Dorko K, Kumer SC, Schmitt TM, et al. (2014) Mechanisms of acetaminophen-induced cell death in primary human hepatocytes. Toxicology and applied pharmacology 279: 266-274.

81. McGill MR, Sharpe MR, Williams CD, Taha M, Curry SC, et al. (2012) The mechanism underlying acetaminophen-induced hepatotoxicity in humans and mice involves mitochondrial damage and nuclear DNA fragmentation. The

Journal of clinical investigation 122: 1574-1583.

82. Mehta K, Van Thiel DH, Shah N, Mobarhan S (2002) Nonalcoholic fatty liver disease: pathogenesis and the role of antioxidants. Nutrition reviews 60: 289-293.

83. Grinberg L, Fibach E, Amer J, Atlas D (2005) N-acetylcysteine amide, a novel cell-permeating thiol, restores cellular glutathione and protects human red blood cells from oxidative stress. Free Radical Biology and Medicine 38(1): 136-145.

84. Niki E (2014) Role of vitamin E as a lipid-soluble peroxyl radical scavenger: in vitro and in vivo evidence. Free Radical Biology and Medicine 66: 3-12.

Figure 2.1. THS exposure results in oxidative stress in the liver. (A) Schematic depicting basic oxidative stress response in cells. **(B)** THS-exposed mice have increased SOD enzymatic activity compared to control mice. **(C)** THS-exposed mice show increased hydrogen peroxide in the liver compared to control mice. **(D)** THS-exposed mice do not show significant decrease in catalase enzymatic activity compared to control **(E)** THS-exposed mice also do not show a significant difference in GPx activity compared to control mice. *All data are Mean ± SD* *= $p < 0.05$ *NS= Not statistically significant.* n=6. *P values were adjusted for the number of times each test was run.*

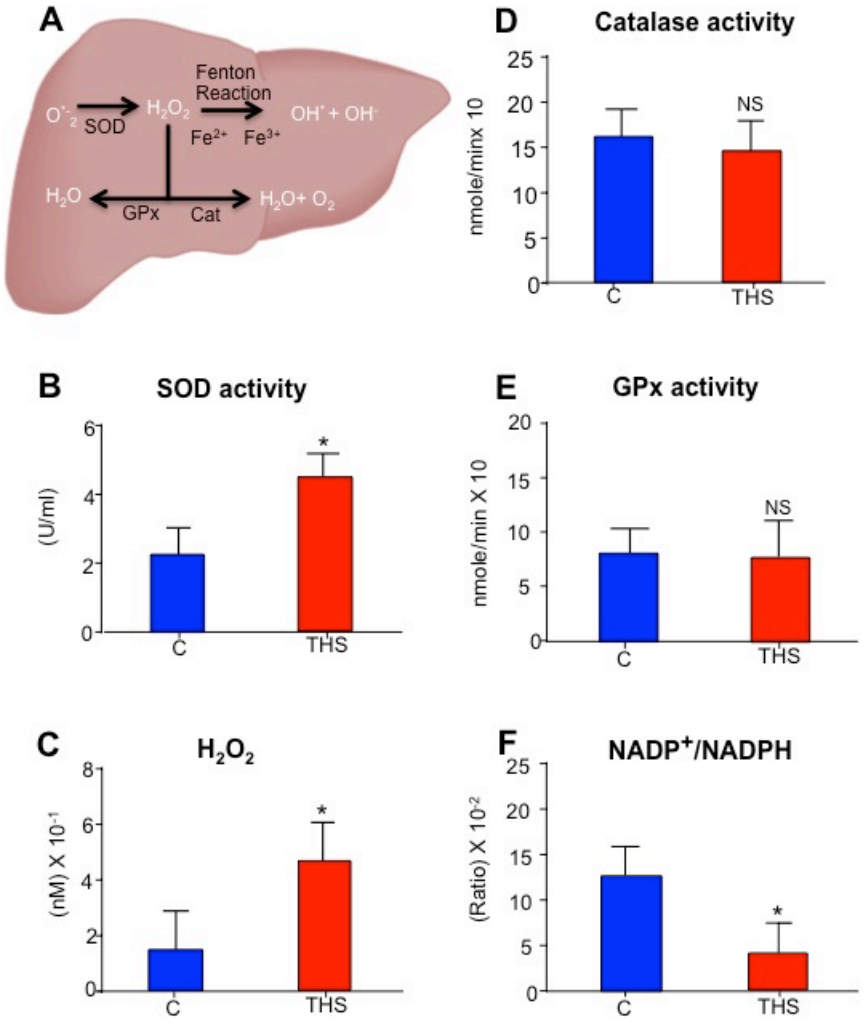
A
Fenton
Reaction
SOD
Fe2+ Fe3+
GPx
Cat
B
SOD activity
(U/ml)
C
THS
C
H2O2
(nM) X 10-1
*
D
Catalase activity
nmole/minx 10
NS
E
GPx activity
nmole/min X 10
F
NADP+/NADPH
(Ratio) X 10-2

Figure 2.1

Figure 2.2. THS exposure increase oxidative stress mediated damage. (A) Model of oxidative stress induced mediated damage in cells. **(B)** THS-exposed mice have higher lipid peroxidation in the liver compared to control mice **(C)** THS-exposed mice show higher protein nitrosylation in the liver compared to control mice **(D)** THS-exposed mice exhibit higher DNA damage in the liver compared to control. **(E)** THS toxins also decrease ATP levels, **(F)** increase AST levels and urea in THS exposed mice **(G).** *All data are Mean ± SD* ***=** $p < 0.05$ *NS= Not statistically significant*. n= 8 for **B,C,** and **D**. n=6 for **E-G**. *P values were adjusted for the number of times each test was run.*

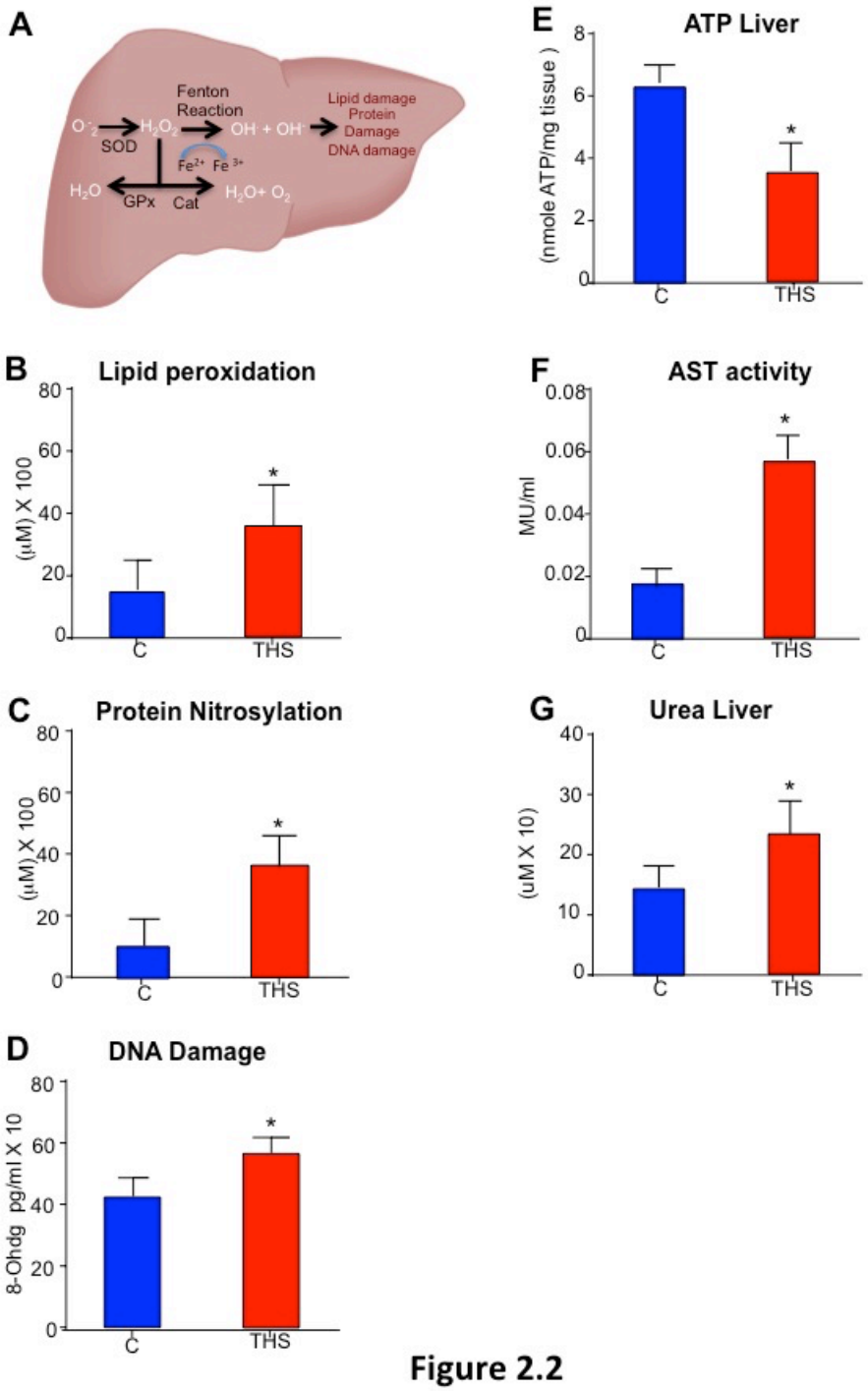
A
Fenton Reaction
SOD
GPx
Cat
Lipid damage
Protein Damage
DNA damage
B
Lipid peroxidation
(µM) X 100
C
THS
C
Protein Nitrosylation
(µM) X 100
D
DNA Damage
8-Ohdg pg/ml X 10
E
ATP Liver
(nmole ATP/mg tissue)
F
AST activity
MU/ml
G
Urea Liver
(uM X 10)

Figure 2.2

Figure 2.3. Antioxidant treatment leads to improvement oxidative stress in the liver of THS-exposed mice. (A) THS-exposed mice treated with the NAC+ α-TOC have significantly reduced of SOD activity and **(B)** low levels of H_2O_2. **(C)** NAC+α-TOC treatment has no significant change in the enzymatic activity of catalase in THS-exposed mice **(D)** NAC+ α-TOC treatment also did not led to a significant change in the enzymatic activity of GPx but it resulted in (**E)** significant increase of NADP+/NADPH ratio in THS exposed mice. *All data are Mean ± SD* ***=** $p < 0.05$ *NS= Not statistically significant* n= 9 for A and E n= 8 for B,C, and D. *P values were adjusted for the number of times each test was run.*

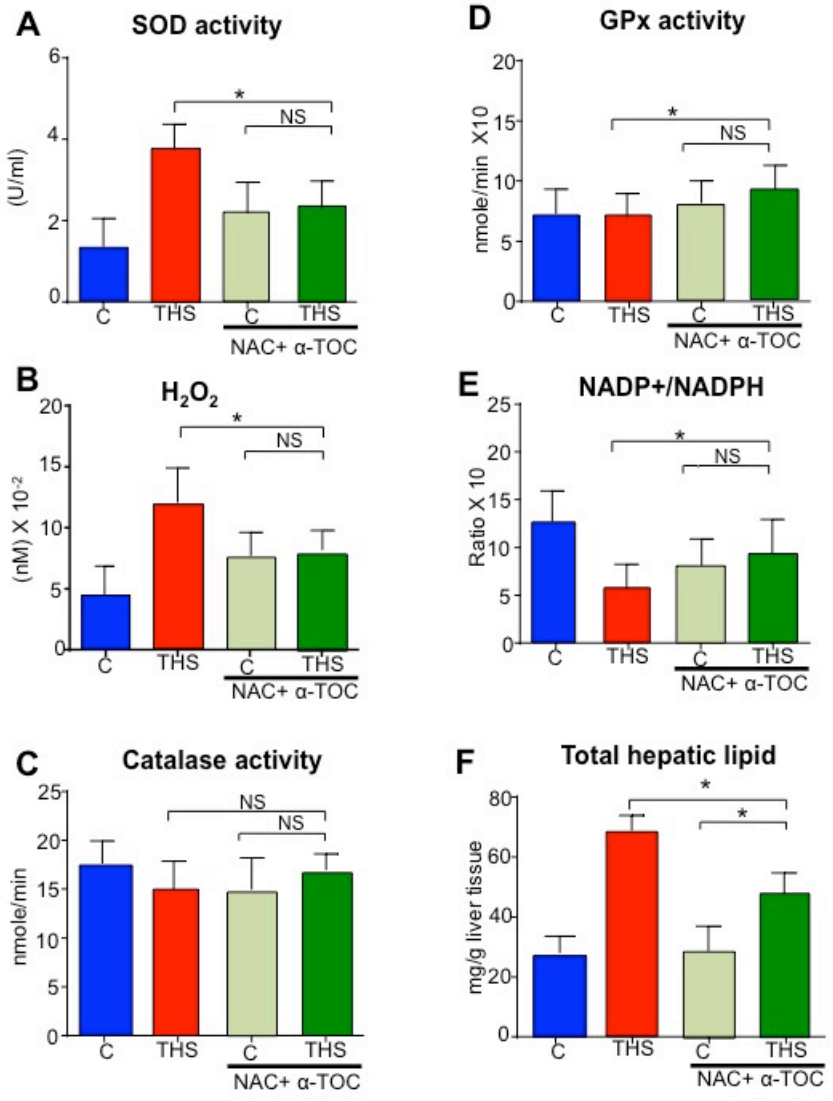
A
SOD activity
(U/ml)
6
4
2
0
*
NS
C
THS
C
THS
NAC+ α-TOC
D
GPx activity
nmole/min X10
20
15
10
5
0
*
NS
C
THS
C
THS
NAC+ α-TOC
B
H2O2
(nM) X 10-2
20
15
10
5
0
*
NS
C
THS
C
THS
NAC+ α-TOC
E
NADP+/NADPH
Ratio X 10
25
20
15
10
5
0
*
NS
C
THS
C
THS
NAC+ α-TOC
C
Catalase activity
nmole/min
25
20
15
10
5
0
NS
NS
C
THS
C
THS
NAC+ α-TOC
F
Total hepatic lipid
mg/g liver tissue
80
60
40
20
0
*
*
C
THS
C
THS
NAC+ α-TOC

Figure 2.3

Figure 2.4. Oxidative stress mediated damage is improved by treating the mice with antioxidants (A) THS-exposed mice treated with NAC+ α-TOC show lower lipid peroxidation **(B)** THS-exposed mice treated with NAC+ α-TOC also show lower protein nitrosylation but **(C)** no significant difference in DNA damage. **(D)** THS-exposed mice treated with NAC+ α-TOC do not have a significant increase in ATP levels, or **(E)** AST levels or **(F)** urea levels. *All data are Mean ± SD* ***=** $p< 0.05$, *NS= Not statistically significant.* n=8 for A n=7 for B n=9 for C,D E,F. *P values were adjusted for the number of times each test was run.*

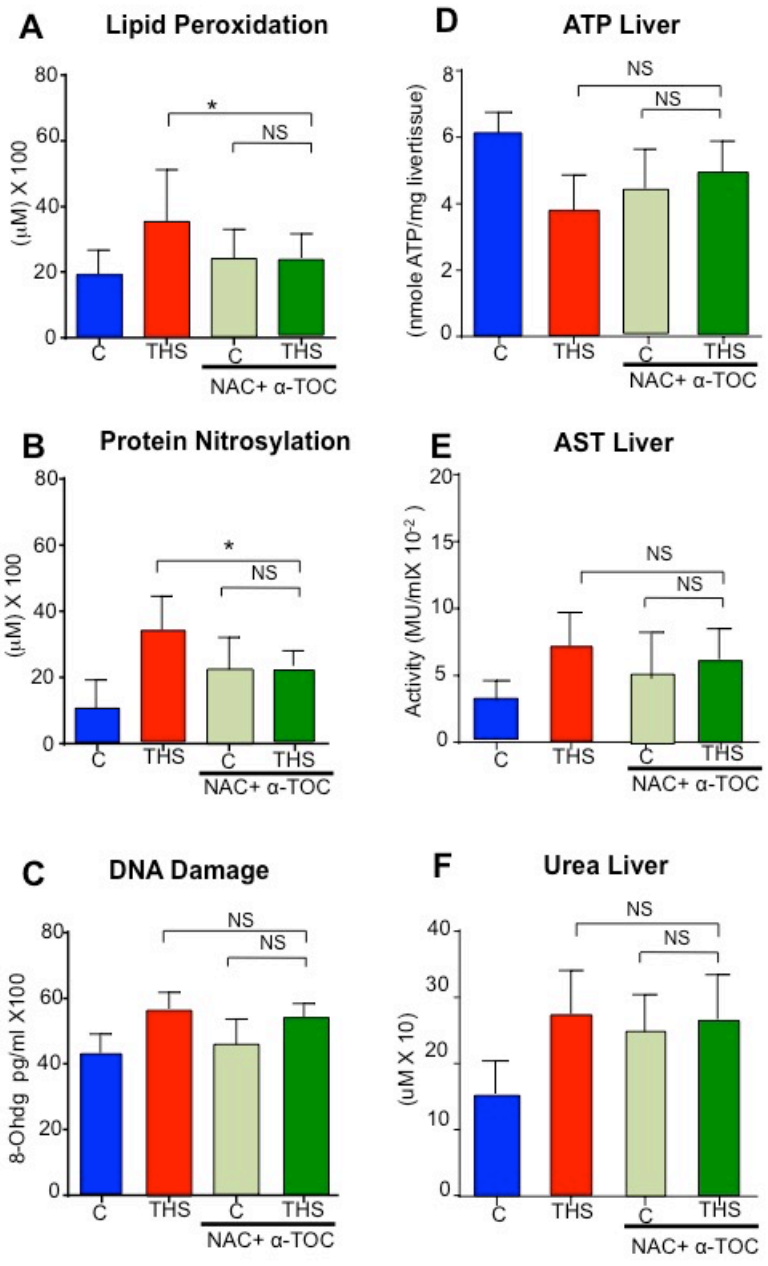
A
Lipid Peroxidation
(μM) X 100
80
60
40
20
0
*
NS
C
THS
C
THS
NAC+ α-TOC
D
ATP Liver
(nmole ATP/mg livertissue)
8
6
4
2
0
NS
NS
C
THS
C
THS
NAC+ α-TOC
B
Protein Nitrosylation
(μM) X 100
80
60
40
20
0
*
NS
C
THS
C
THS
NAC+ α-TOC
E
AST Liver
Activity (MU/mlX 10-2)
20
15
10
5
0
NS
NS
C
THS
C
THS
NAC+ α-TOC
C
DNA Damage
8-Ohdg pg/ml X100
80
60
40
20
0
NS
NS
C
THS
C
THS
NAC+ α-TOC
F
Urea Liver
(uM X 10)
40
30
20
10
0
NS
NS
C
THS
C
THS
NAC+ α-TOC

Figure 2.4

Figure 2.5. APAP treatment results in increase of oxidative stress in THS-exposed mice. (A) APAP treatment results in higher SOD activity in THS-exposed mice. **(B)** APAP treatment also results in higher levels of hydrogen peroxide in THS-exposed mice **(C)** APAP treatment also resulted in a decrease in catalase activity but no significant change in **(D)** GPx activity.**(E)** APAP treatment also did not had a significant impact in the $NADP^+$/NAPPH ratio. *All data are Mean ± SD* ***=** $p< 0.05$ *NS= Not statistically significant* n= 9 for A and E n= 8 for B,C, and D. *P values were adjusted for the number of times each test was run.*

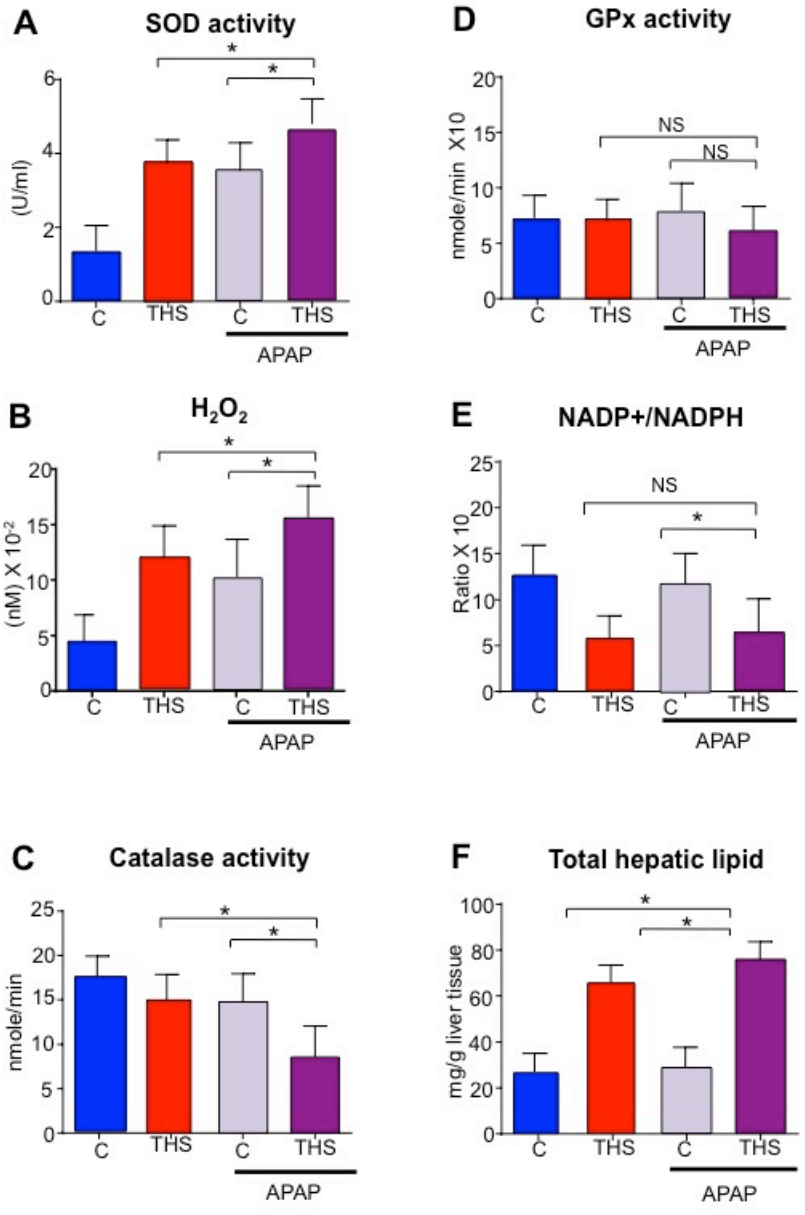
A
SOD activity
(U/ml)
C
THS
C
THS
APAP
D
GPx activity
nmole/min X10
NS
NS
B
H_2O_2
(nM) X 10^{-2}
E
NADP+/NADPH
Ratio X 10
C
Catalase activity
nmole/min
F
Total hepatic lipid
mg/g liver tissue

Figure 2.5

Figure 2.6. THS-exposed mice treatment with APAP increases oxidative stress mediated damage **(A)** APAP treatment results in higher lipid peroxidation, **(B)** higher protein nitrosylation, and **(C)** higher DNA damage in the liver of THS exposed mice. **(D)** THS-exposed mice treated with APAP also have lower ATP levels; **(E)** higher AST levels but **(F)** lower urea levels than THS-exposed mice. *All data are Mean ± SD* *= p< 0.05, *NS= Not statistically significant.* n=8 for A n=7 for B n=9 for C,D E,F. *P values were adjusted for the number of times each test was run.*

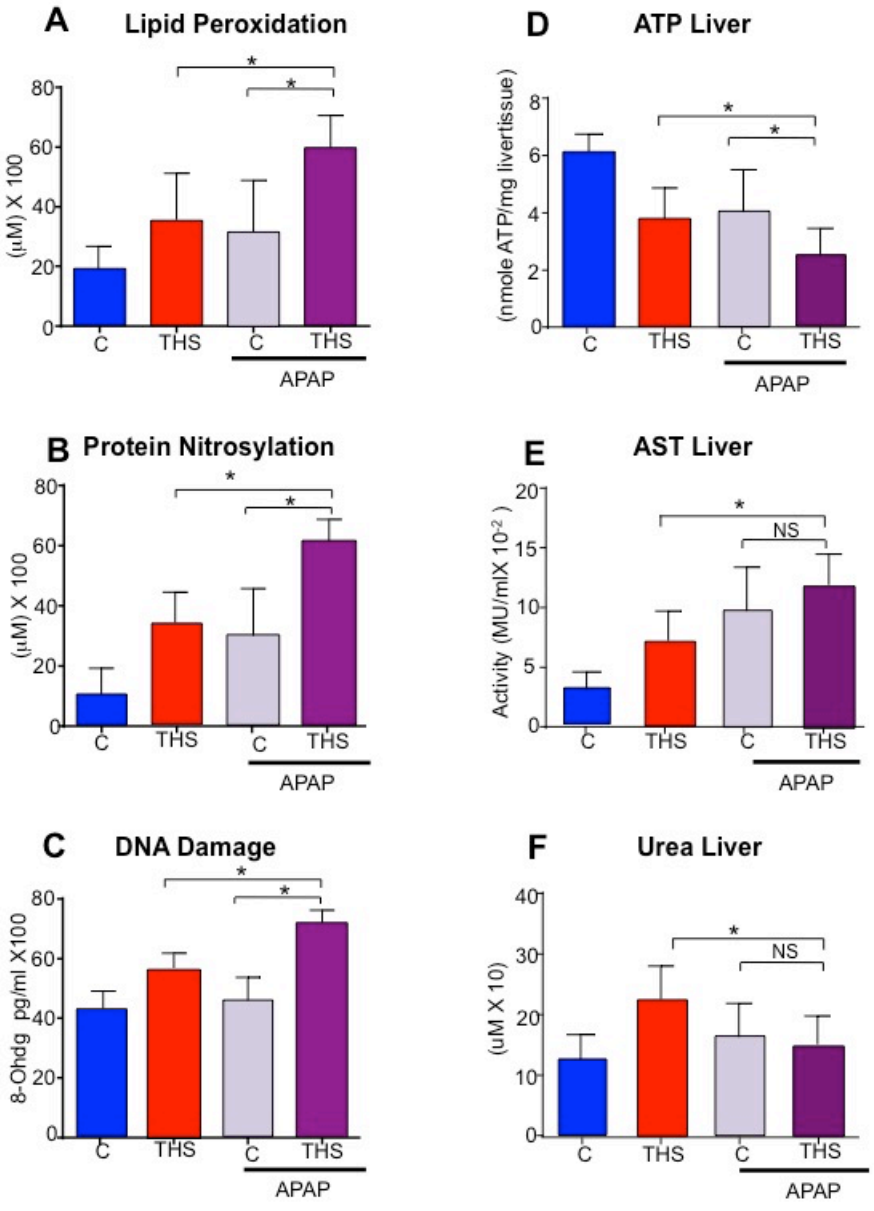
A
Lipid Peroxidation
(µM) X 100
0
20
40
60
80
C
THS
C
THS
APAP
*
*
B
Protein Nitrosylation
(µM) X 100
0
20
40
60
80
C
THS
C
THS
APAP
*
*
C
DNA Damage
8-Ohdg pg/ml X100
0
20
40
60
80
C
THS
C
THS
APAP
*
*
D
ATP Liver
(nmole ATP/mg livertissue)
0
2
4
6
8
C
THS
C
THS
APAP
*
*
E
AST Liver
Activity (MU/mlX 10-2)
0
5
10
15
20
C
THS
C
THS
APAP
*
NS
F
Urea Liver
(uM X 10)
0
10
20
30
40
C
THS
C
THS
APAP
*
NS

Figure 2.6

Figure 2.7. THS toxins alter SIRT1/AMPK/ SBREP1c signaling in the liver.

(A) Antioxidant treatment and THS exposure results significant lower total lipid hepatic weight in THS-exposed mice. **(B)** APAP treatment in conjunction of THS exposure also results in higher total lipid hepatic weight. **(C)** THS-exposed mice have less SIRT1 levels than controls, **(D)** lower AMPK-P levels and **(E)** higher levels of SREBP1c than control mice. *= $p< 0.05$, ** $p<0.01$ *NS= Not statistically significant.* n=6 *P values were adjusted for the number of times each test was run. "Fold change" on western blot quantification graph indicate fold change to control.*

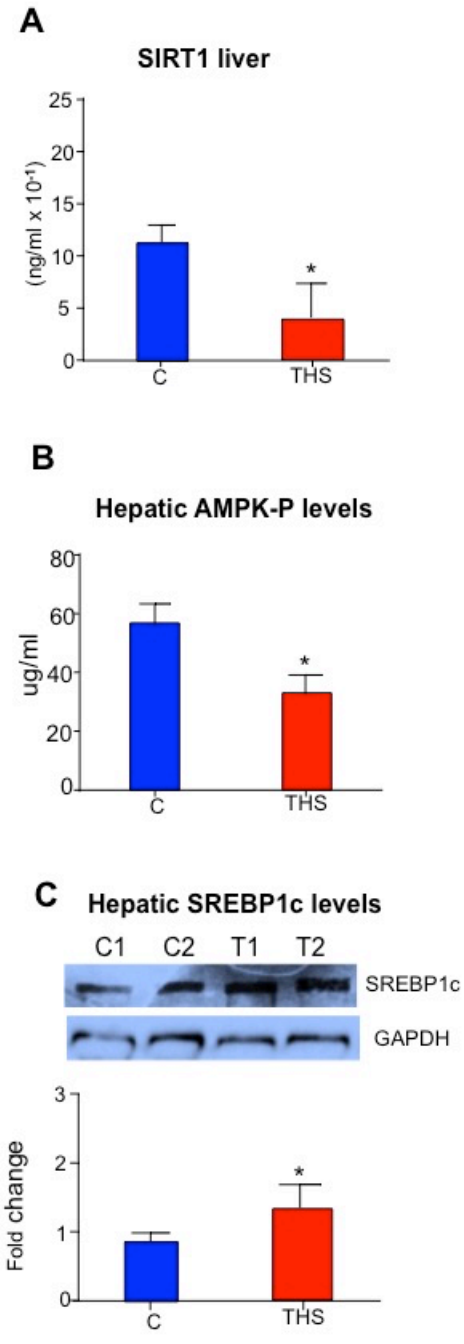
A
SIRT1 liver
(ng/ml x 10-1)
25
20
15
10
5
0
*
C
THS
B
Hepatic AMPK-P levels
ug/ml
80
60
40
20
0
*
C
THS
C
Hepatic SREBP1c levels
C1
C2
T1
T2
SREBP1c
GAPDH
Fold change
3
2
1
0
*
C
THS

Figure 2.7

Figure 2.8. Proposed working model of THS-induced hepatic steatosis. A schematic representation of THS-induced hepatic steatosis in mice depicting how THS toxins increases oxidative stress in the liver, which results in decrease of SIRT1 levels, a key regulator oxidative stress and regulate lipid metabolism. The toxins also result in a decrease in the levels of active AMPK and increase in SREBP1c levels, key regulator of *de novo* lipid metabolism. As a result THS exposure induces fat accumulation in the liver which results in hepatic steatosis.

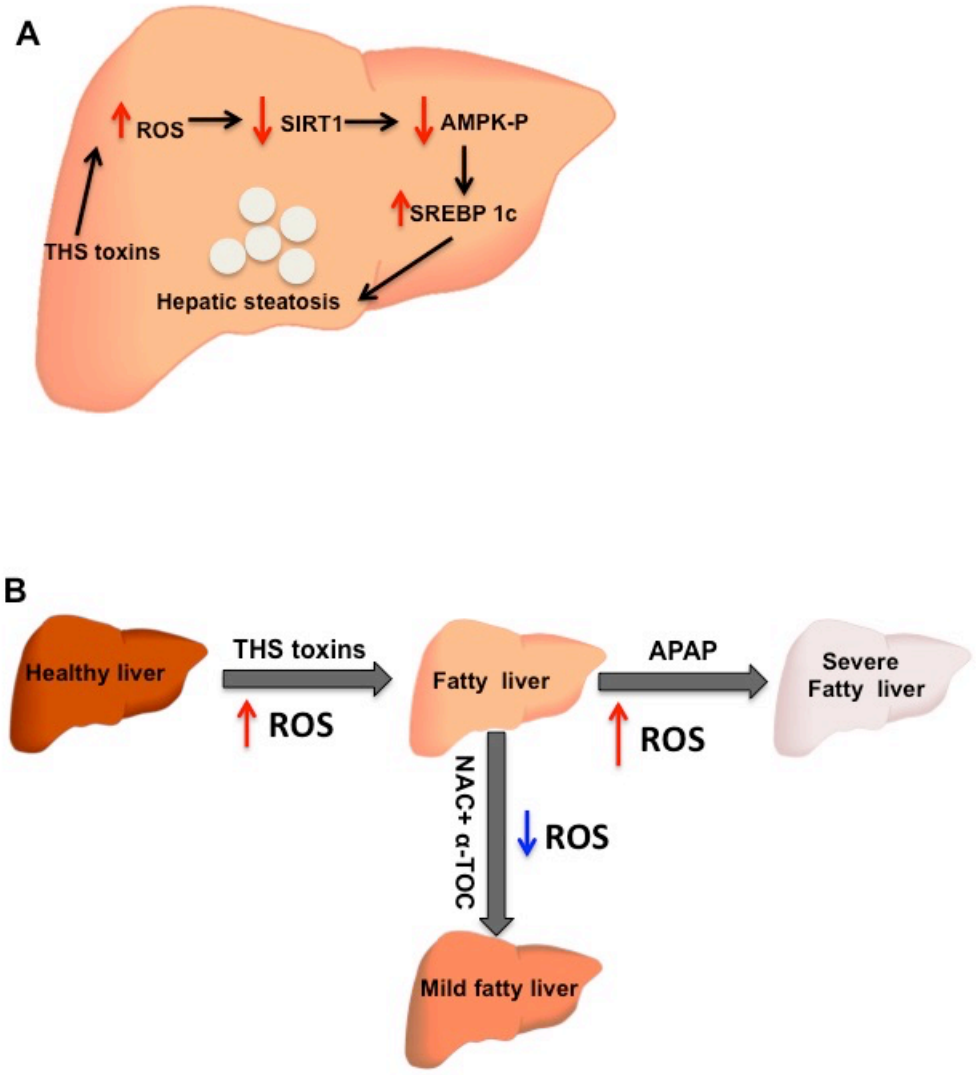
A
ROS
SIRT1
AMPK-P
SREBP 1c
THS toxins
Hepatic steatosis
B
Healthy liver
THS toxins
ROS
Fatty liver
APAP
ROS
Severe
Fatty liver
NAC+ α-TOC
ROS
Mild fatty liver

Figure 2.8

Figure S1. Immunolabeling for lipid peroxidation. Representative images of liver tissue staining for 4-HNE lipid peroxidation adducts. Livers of control mice have less lipid peroxidation than control livers.

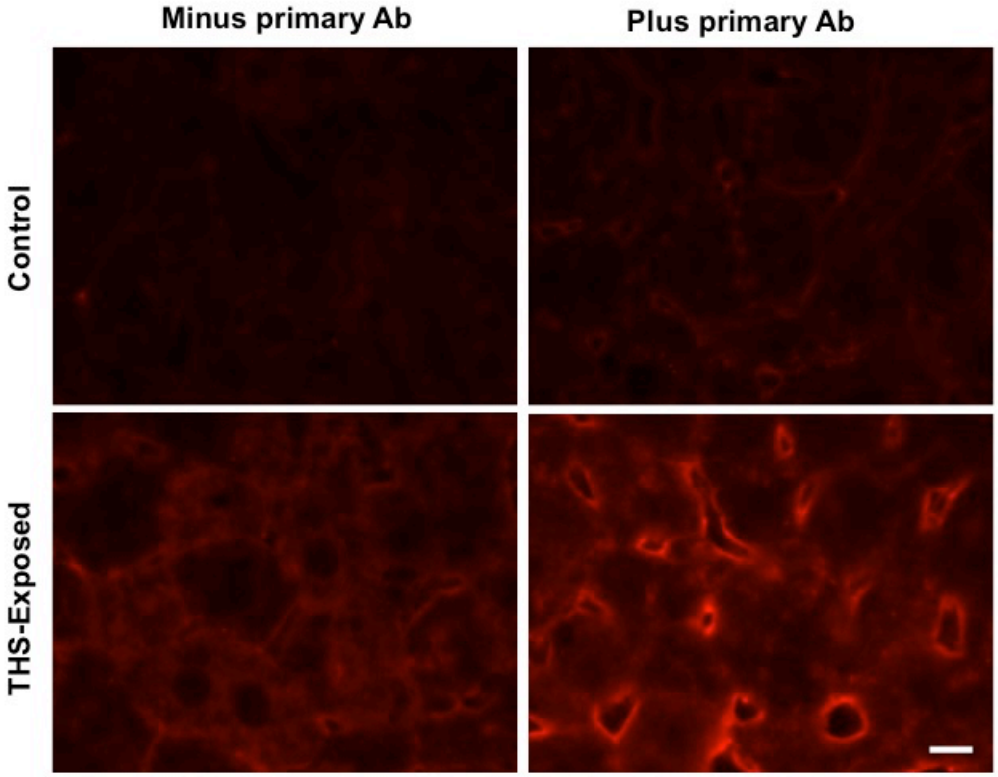

Figure S1

CHAPTER 3:

The role of fatty acid metabolism and apolipoproteins in THS-induced hepatic steatosis in mice

Abstract

Background: Hepatic steatosis results from the increase of accumulation of lipids in the liver, decrease of beta fatty acid oxidation and/or decrease in the export to peripheral tissue by apolipoproteins. Previously, we showed that THS toxins result in hepatic steatosis in mice.

Objective: The goal of this paper was two-fold: (1) To determine whether THS toxins alter key molecules involved in beta fatty acid metabolism and (2) to determine whether the levels of apolipoprotein B is decreased in THS-exposed mice leading to decrease export of lipid from the liver.

Methodology: Mice were exposed to THS toxins for 6 months before performing the studies shown here. THS-exposed mice were also placed on western diet for five months or treated with AICAR to determine how THS-toxins affect the lipid metabolism of these animals.

Results: THS-exposed mice do not show significant difference in the levels of key fatty acid metabolism enzymes (CPT1, ACC, IDH2 and LCAD) compared to the control, suggesting THS toxins do not decrease the levels of these enzymes. THS-exposed mice have lower levels of SIRT3 and ATP. These mice also have lower IDH2 activity. THS-exposed mice also have lower levels of apolipoprotein B compared to control, suggesting the excess fatty acids, which are converted to TG in the liver, are not being transported to peripheral tissue for usage or storage.

Conclusion: These results suggest that even thought THS toxins do not alter the levels of fatty acid metabolism enzymes, exposure result in lower levels of SIRT3 and lower IDH2

activity resulting in lower production of ATP in THS-exposed mice. THS toxins exposure also decrease of transport of lipids out of the liver by decreasing the levels of apolipoprotein B. Consequently, THS-exposed mice have an increase in lipid accumulation in the liver resulting in hepatic steatosis.

Introduction

The liver is one of the largest and most metabolically active organs in the body. In addition to performing a myriad of metabolic functions that regulate energy levels, the liver is a major site for protein synthesis and is responsible for the production of lipids to be delivered to other tissues [1-2]. Under normal conditions, the liver is constantly regulating synthesis and breakdown of lipids to meet physiological metabolic demands. In the liver, AMPK and SREBP1c regulate the synthesis of lipids in the liver. When there is an excess of fatty acids in the liver, SREBP1c is activated and activates acetyl-coA carboxylase (ACC), which leads to the activation of malonyl CoA, resulting in the synthesis of triglycerides (TGs) [4-8]. If not secreted into circulation, these TGs accumulate in the liver and can result in hepatic steatosis. Conversely, the liver can increase breakdown of fatty acids via beta-oxidation to decrease lipid accumulation by decreasing the activation of SREBP1c and increasing the activation of key mitochondrial enzymes that participate in the oxidation of fatty acids, such as carnitine palmitoyltransferase I (CPT1), long-chain acyl-CoA dehydrogenases (LCAD), and isocitrate dehydrogenase 2 (IDH2). These enzymes catalyze fatty acid breakdown starting by transporting the activated fatty acids into the mitochondria by CPT1. LCAD then further processes the fatty acids that enter the tricarboxylic acid (TCA) cycle in the form of acetyl-CoA. The processing of the fatty acids continues via the participation of IDH2, which allows the fatty acids to be converted into high-energy molecules that can be used for the synthesis of ATP during oxidative phosphorylation. Therefore, low ATP production can be a result of a decrease in levels or function of LCAD or IDH2 [9-14].

Perturbation of this catabolic pathway can result in abnormal fatty acid metabolism, which can consequently lead to the accumulation of lipids in the hepatocytes, resulting in hepatic steatosis.

Another path by which the hepatocytes can further control lipid accumulation is by transporting excess lipids out of the liver by increasing very low density lipoprotein (VLDL) assembly and secretion. A decrease in VLDL assembly and secretion has been associated with hepatic steatosis [15-17]. VLDL particles, which are synthesized in the liver, are responsible for delivering TGs to the different cells of the body. VLDL particles are composed of TG, cholesterol and apolipoprotein (apoB). In the liver, VLDL synthesis is greatly affected by the levels of microsomal triglyceride transfer protein (MTTP) and apoB [18-26]. ApoB in particular has been associated with non-alcoholic fatty liver (NAFLD). Past studies have shown that insulin has the ability to inhibit the expression of apoB, whereas fatty acids induce its expression [20-21]. Also, patients with NAFLD have reduced expression of apoB, suggesting that their liver is unable to transport TG into peripheral tissue, resulting in accumulation of lipids in the hepatocytes [18]. The function of apoB is affected by MTTP proteins which allow apoB to be released from the ER and start participating in the organization of the VLDL particles. Low levels of MTTP have also been associated with the degradation of apoB and the decrease of VLDL particles [23-26]. Therefore, altering the level of MTTP and apoB in the liver affects the transport of lipids out of the liver. Consequently, lipid accumulation results in hepatic steatosis.

The ability of the liver to process fatty acids and transport lipids to other tissues is

affected by toxins, diet and drugs [27-34]. Previously, we have shown that exposure to THS toxins results in lipid accumulation in hepatocytes of exposed mice. Recently, we have shown that these mice also have high levels of oxidative stress that lead to lung and liver damage as well as abnormal cognitive behavior [3]. We also showed that THS toxins result in altering the SIRT1/AMPK/SREPB1c pathway [34]. Modulating the levels of oxidative stress with APAP (Tylenol) and antioxidants resulted in worsening and improvement of hepatic steatosis, respectively, in mice exposed to THS toxins. These findings suggested that THS toxins result in hepatic damage by altering the oxidative stress levels and increasing lipid synthesis. The goal of this study is to determine whether THS also affects fatty acid metabolism and lipid transport. Our results show that THS toxins decrease the activity of IDH2 leading to decrease in lipid breakdown and ATP production and that they also decrease the levels of MTTP and apoB, suggesting alterations in the lipid transport system. Our findings show that THS toxins affect the metabolism and transport of lipids in mice while highlighting the danger of THS toxins for liver health.

Materials and methods

Animals: All male C57BL/6 mice used for these experimental procedures were housed under the following environmental conditions: 12-hour light/dark cycle in convectional cages with *ad libitum.* The regular standard chow diet was composed of 58% carbohydrates, 28.5% protein, 13.5% fat and water.

Ethics Statement: The experiments were done according to animal protocols that were approved by the University of California, Riverside, Institutional Animal Care and Use Committee (UCR-IACUC). The mice used for these studies were euthanized by carbon dioxide (CO_2) inhalation, which is the most common method of euthanasia used by NIH. The amount and length of CO_2 exposure were approved by UCR-IACUC.

THS exposure method: The THS exposure method used for these studies has been previously described in detail (3). C57BL 6J mice were housed in THS-exposed material to study the effects of toxins in liver health for a period of 24 weeks. THS exposure of the material (10 g curtain composed of cotton, 10 g upholstery composed of cotton and 10 g carpet composed mainly of fiber) was done using a Teague smoking apparatus. The machine was set to smoke two packs of 3R4F research cigarettes five days a week to model a regular smoker (cigarette/15 min). The total particulate matter (TPM) was set to 30μg/m^3, which is the TPM found in the homes of smokers. The mice were housed in the TSH-exposed material for a week and the material was exposed for four weeks to allow the toxins to age. After four weeks the material was discarded. The control C57BL 6J

mice were not exposed to THS toxins and were housed in a different room than the THS-exposed mice.

Western Diet treatment: After weaning, normal C57 BL/6J male mice and Third-Hand Smoke (THS)-exposed C57 BL/6J male mice were placed on a western chow diet for duration of 6 months. The western diet was purchased from Harlan laboratories (Cat# TD88137) and was composed of 21% anhydrous milk fat (butterfat), 34% sucrose, and 0.2% cholesterol.

AICAR treatment: AICAR was purchased from Toronto Research Chemicals (Cat# A440500) and was dissolved in phosphate buffered saline (PBS). THS-exposed or control mice were given an intraperitoneal injection (I.P) of either AICAR (250 mg/kg for 5 days/week) or a comparable volume of PBS for eight weeks.

Tissue Extracts: After six months of THS exposure, the livers of THS-exposed male mice were extracted and immediately frozen and stored at -80°C. Protein extracts were made from portions of the frozen tissue unless otherwise specified by the kits' instruction manuals, and were used for ELISA analysis. Liver tissue was homogenized in radioimmunoprecipitation assay buffer (RIPA), centrifuged, and the supernatant collected unless otherwise specified by the kits' instruction manuals.

Blood Extracts: Blood was extracted directly from the heart and allowed to coagulate for 20-30 min. The samples were then centrifuged at 2000 RPM to induce phase separation between plasma proteins and serum. The serum was then collected from the blood samples. The serum was used immediately for assays or immediately frozen and stored at -80° C.

Total lipid: Lipid content in the liver was determined using the Folch method (7). Tissue was homogenized with chloroform/methanol (2/1) to a final volume 20 times the volume of the tissue sample and agitated for 15-20 min. The homogenate was centrifuged to recover the liquid phase. The solvent was washed with 0.2 volume of 0.9% NaCl solution. After vortexing, the mixture was centrifuged at 2000 RPM to separate the two phases. The upper phase was removed and the lower chloroform phase containing lipids was evaporated under vacuum in a rotary evaporator. To determine the total amount lipids in the sample the weight of the vial was subtracted from the weight of the vial plus lipids.

Measurement of fatty acids (FA) levels: Fatty acids were quantified using Abcam kits (Cat #ab65341). In this assay, FAs are converted to their CoA derivatives and subsequently oxidized, leading to formation of color/fluorescence. Fatty acid levels were quantified using the absorbance values obtained from the liver tissue homogenates samples at 550 nm.

Measurement of triglyceride (TG) levels: The TG contents were measured using Cayman Triglyceride Colorimetric Assay Kit (Cat# 10010303). The Triglyceride

Colorimetric Assay uses the enzymatic hydrolysis of triglycerides by lipase to produce glycerol and free fatty acids. The absorbance of standards and samples were read at 550 nm. Absorbance values were used to generate a standard curve. The levels of TG were interpolated from this standard curve.

Measurement of IDH2 levels: The IDH2 levels in liver of THS-exposed mice were quantified using IDH2 ELISA kit from Mybiosource (Cat# MBS074031). IDH2 levels were quantified by incubation of tissue homogenate in an anti-IDH2 antibody coated plate, followed by an HRP conjugated secondary antibody. The optical density (O.D.) of the samples was then read at 450 nm. The values were used to quantify the levels of IDH2 in each sample.

Measurement of LCAD levels: The LCAD levels in THS-exposed mice were quantified using the ELISA kit from Mybiosource (Cat# MBS931062). LCAD levels were quantified by incubation of tissue homogenate in an anti-LCAD antibody coated plate, followed by an HRP conjugated secondary antibody. The optical density O.D. of the plate was then read at 450 nm. The values were used to quantify the levels of LCAD in the liver.

Measurement of CPT1 levels: The CPT1 levels of THS-exposed mice were quantified using CPT1 ELISA kit from Mybiosource (cat# MBS7252964). CPT1 levels were quantified by incubation of tissue homogenate in an anti-CPT1C antibody coated plate followed by detection by substrate solution provided in the kit. The O.D. of the plate was then read at 450 nm. The values were used to quantify the levels of CPT1 in each sample.

Measurement of ACC levels: ACC levels were determined using an ELISA kit from Mybiosource (Cat# MBS2606160). ACC levels were quantified by incubation of liver tissue homogenate in an anti-ACC antibody coated plate, by detection by substrate solution provided in the kit. The O.D. of each well was measured at 450 nm. The resulting O.D. values were used to calculate the ACC levels in the liver.

Measurement of apoB levels: The apoB levels in liver of THS-exposed mice were quantified using apoB ELISA kit from Neoscientific (Cat# MA0520). APOB levels were quantified by incubation of tissue homogenate in an anti-apoB antibody coated plate. The O.D. f the plate was then read at 450 nm. The values were used to quantify the standard curve, which was used to calculate the levels of apoB in the liver samples.

Measurement of MTTP levels: MTTP levels in the livers of THS-exposed mice were quantified using MTTP ELISA kit from Mybiosource (Cat# MBS9329329). MTTP levels were quantified by incubation of tissue homogenate in an anti-MTTP antibody coated plate, followed by an HRP conjugated secondary antibody. The optical density O.D. of the plate was then read at 450 nm. The values were used to generate a standard curve and to quantify the levels of MTTP in the liver.

Measurement of VLDL levels: VLDL levels in the livers of THS-exposed mice were quantified using VLDL ELISA kit from Mybiosource (Cat# MBS706037). VLDL levels were quantified by incubation of tissue homogenate in an anti-VLDL antibody coated plate, followed by an HRP conjugated secondary antibody. A standard curve was

generated and used to quantify VLDL levels in liver tissue of THS-exposed mice and control mice.

Statistical Analysis: For the statistical analysis of experiments mentioned above, we used Graphpad Instat Software (Graphpad, La Jolla, CA, USA). Statistical comparisons between two-groups was performed using the unpaired Student's *t*-test. All data are mean±SD represented by the error bars. Means among samples were considered significantly different when $p<0.05$.

Results

Hepatic steatosis can result from an increase of *de novo* lipid synthesis, decrease of breakdown of fatty acids, or decrease of the transport of lipids out of the liver. Previously, we showed that THS toxins increase oxidative stress in the liver of mice resulting in hepatic steatosis [34]. In this study we investigated whether THS-exposure changes the levels and/or activity of key enzymes involved in the breakdown of fatty acids and in the transport of lipids out of the liver.

THS-exposure affects FA, TG and total lipid levels in the liver

Quantification of fatty acids, TG and lipids in THS-exposed mice showed higher levels of all three in the liver of THS-exposed mice (**Figure 3.1A-C**). Because western diet (WD), which is rich in fat (see Materials and Methods section) and has been shown to decrease the activation of AMPK, an enzyme that regulates the breakdown of fatty acids in the liver [35], we tested whether WD augments the effects caused by THS-exposure. Mice were placed at weaning (3 weeks of age) on WD in conjunction with THS exposure for 5 months. At the end of this period we analyzed again for FA, TG and total hepatic lipids and found that none of these parameters were significantly higher when compared to the mice on the chow diet and exposed to THS (**Figure 3.2A-C**). However, there was a significant difference in the levels compared to those of mice feed WD only (**Figure 3.2A-C**).

To investigate whether an stimulator of AMPK phosphorylation, 5-aminoimidazole-4-carboxamide-1-beta-4-ribofuranoside (AICAR) [35], resulted in

improved fatty acid metabolism in the THS-exposed mice, we treated mice exposed to THS for 6 months with AICAR at 250 mg/kg for 5 days/week for eight weeks via an intraperitoneal injection and treated the controls in a similar way with comparable volume of PBS. Indeed, we found that AICAR was able to reverse the adverse effects of THS exposure in lipid metabolism. The levels of fatty acids, TG and total lipids were returned to normal levels even in the presence of THS exposure (**Figure 3.3 A-C**).

Effects of THS-exposure on the levels/activity of enzymes involved in fatty acid metabolism.

Based on the results presented above we examined whether THS-exposure affects the levels of key enzymes that play a role in the breakdown of fatty acids in the liver. For these studies we measured the levels of Acetyl-CoA carboxylase (ACC), carnitine palmitoyltransferase I (CPT1), long-chain acyl-CoA dehydrogenases (LCAD), and isocitrate dehydrogenase 2 (IDH2) after six months of exposure. Except for IDH2, that we found to have a tendency to be decreased, the other three enzymes did not show levels different from the control and the THS-exposed mice (**Figure 3.4A-D**). Because, we observed that IDH2 levels were consistently lower in THS-exposed mice although be it not quite significantly lower, we tested for activity of IDH2 and found that its activity is significantly decreased in THS-exposed mice (**Figure 3.5A**).

Because it is known that SIRT3 plays a key role in fatty acid metabolism and that it modulates the activity of IDH2, we examined the levels of SIRT3 in THS-exposed mice. We found lower levels of SIRT3 in the liver of THS-exposed mice when compared

to the control suggesting that these mice might have lower fatty acid breakdown than the controls (**Figure 3.5B**). Because IDH2 is an important enzyme in the TCA cycle, which is key for the production of the reduction potential in the cell (NADPH an FADH2), which then provides the electrons to the oxidative phosphorylation chain to produce ATP, we measured the level of ATP to determine whether it was affected by THS exposure. We found that ATP levels were significantly reduced in the liver of THS-exposed mice (**Figure 3.5C**). Taken together these results suggest that the capacity of lipids to undergo b-oxidation in the liver is reduced by THS- exposure, which very likely leads to the accumulation of lipids in the hepatocytes.

THS exposure results in a decrease of VLDL assembly in the liver.

To determine whether THS-exposure affects lipid transport out of the liver, we investigated whether THS toxins alter the level of proteins involved in lipid transport out of the liver. Both apolipoprotein B (apoB) and microsomal triglyceride transfer protein (MTTP) have been associated with the transport of lipids out of the liver into peripheral tissues such as to the adipose tissue. We focused on apoB and MTTP because these proteins play a key role in VLDL assembly, a particle type that is critical in transport of lipids out of the liver [23-26]. THS-exposed mice showed lower levels of apoB (**Figure 3.6A)** and MTTP (**Figure 3.6B)** in the liver compared to the controls. In addition, we also found that THS-exposed mice had lower VLDL levels than controls (**Figure 3.6C**). These findings indicate that THS toxins alter processes involved in lipid transport out of the liver through decreased levels of VHDL particle formation and consequently this contributes to lipid accumulation in the liver of THS-exposed mice.

Discussion

We have previously shown that THS exposure results hepatic steatosis [3]. More recently we showed that, THS-exposed mice have high levels of hepatic oxidative stress leading to liver damage. We also showed that the lipid accumulation observed in THS-exposed mice is due to increase in the levels of oxidative stress, primarily of ROS, and inhibition of the SIRT1/AMPK/SREBP1c pathway [34]. The goal of this study is to determine whether THS toxins affect fatty acid metabolism and lipid transport in THS-induced hepatic steatosis.

In this study, we show that THS-exposed mice are unable to metabolize and transport lipids efficiently compared to the control mice. These mice have higher lipids, fatty acids and TG suggesting these animals do not have the metabolic efficiency exhibited by the control mice. WD diet has been associated with increase lipid accumulation in the liver whereas AICAR treatment has been associated with a decrease in lipid accumulation [35-40]. Western diet has been shown to increase oxidative stress and increase fat accumulation in the liver by decreasing fatty acid metabolism resulting in hepatic steatosis. THS-exposed mice placed on WD did not have a worse lipid profile than the THS-exposed mice placed on chow diet. However, AICAR treatment led to improved lipid metabolism in THS-exposed mice. THS exposed mice treated with AICAR had lower FA, TG and hepatic lipids. These finding suggest AICAR is able to reverse the lipid abnormalities induced by THS toxins but WD is unable to further worsen the lipid abnormalities triggered by THS toxins.

Fatty acid metabolism plays a key role in the development of hepatic steatosis [33]. In our Previously we showed THS-toxins increase the oxidative stress levels and lower SIRT1 levels (34). Consequently, THS-exposed mice have higher lipid synthesis than the control. In this study we focused on SIRT3 because it is a key regulator of fatty acid breakdown. SIRT3 plays a key role in lipid homeostasis in the liver and by increasing fatty acid metabolism in the mitochondria. This sirtuin also regulates fatty acid metabolism by enhancing the activity of IDH2, which is involved in processing the fatty acids via the TCA cycle in the liver [11-12]. THS-exposed mice show lower levels of SIRT3 as well as lower activity of IDH2 suggesting than THS toxins alter lipid metabolism by also targeting the breakdown of fatty acids in the mitochondria. Consequently, THS-exposed mice do not have the same metabolic efficiency as the controls; they have less fatty acid breakdown and more lipid accumulation in the liver than controls.

Hepatic steatosis can also result from abnormal lipid transport. We were able to show that THS toxins result in a decrease in the expression and levels of apoB and MTTP, two key molecules involved in the assembly of VLDL particles. Apoliproteins play a key role in transporting lipids from one organ to another. ApoB plays a key role in the transport of lipids out of the liver to peripheral tissue [18-26]. Decreasing the levels of this protein results in the decrease of transports of lipids out of the liver and consequently in the accumulation of lipids in the liver. Insulin has been associated with the negative regulation of apoB in the liver. Previously we have showed that THS-exposed mice have insulin resistance and high levels of insulin in the serum. Therefore is possible that

insulin resistance contributes to the low levels of apoB. The regulation of apoB also seems to occur at the transcriptional level since both DNA microarray and RNA-seq show that THS-exposed mice have lower expression levels of apoliproteins relative to the control. To our knowledge this is the first paper that shows that THS toxins causes lipid accumulation in the liver by targeting proteins involved in VLDL assembly (**Figure 3.7A**).

In conclusion, THS toxins decrease SIRT3 levels and IDH2 activity in the liver leading to a decrease in fatty acid metabolism (**Figure 3.7B**). In addition to a lower breakdown of fatty acids, THS-exposed mice also have lower VLDL levels compared to the control mice. These findings are significant because they provide further characterization of THS-induced hepatic steatosis in mice and further insights into the danger of exposure of THS toxins to liver health.

References

1. Bechmann LP, Hannivoort RA, Gerken G, Hotamisligil GS, Trauner M, et al (2012). The interaction of hepatic lipid and glucose metabolism in liver diseases. *Journal of hepatology*, *56*(4), 952-964.

2. Serra D, Mera P, Malandrino MI, Mir JF, Herrero L (2013). Mitochondrial fatty acid oxidation in obesity. *Antioxidants & redox signaling*, *19*(3), 269-284.

3. Martins-Green M, Adhami N, Frankos M, Valdez M, Goodwin B, et al. (2014) Cigarette smoke toxins deposited on surfaces: implications for human health. PloS one 9: E86391.

4. Yuan H, Shyy JYJ, Martins-Green M (2009) Second-hand smoke stimulates lipid accumulation in the liver by modulating AMPK and SREBP-1. J Hepatol 51: 535-547.

5. Jung EJ, Kwon SW, Jung BH, Oh SH, Lee BH (2011) Role of the AMPK/ SREBP-1 pathway in the development of orotic acid-induced fatty liver. J Lipid Res 52: 1617-1625. 71.

6. Ahmed MH, Byrne CD (2007) Modulation of sterol regulatory element binding proteins (SREBPs) as potential treatments for non-alcoholic fatty liver disease (NAFLD). Drug Discov Today 12: 740-747.

7. Kohjima M, Higuchi N, Kato M, Kotoh K, Yoshimoto T et al (2008). SREBP-1c, regulated by the insulin and AMPK signaling pathways, plays a role in nonalcoholic fatty liver disease. *International journal of molecular medicine*, *21*(4), 507-511.

8. Li X, Li Y, Yang W, Xiao C, Fu S et al (2014). SREBP-1c overexpression induces triglycerides accumulation through increasing lipid synthesis and decreasing lipid oxidation and VLDL assembly in bovine hepatocytes. *The Journal of steroid biochemistry and molecular biology*, *143*, 174-182.

9. Hirschey MD, Shimazu T, Goetzman E, Jing E, Schwer B et al (2010). SIRT3 regulates mitochondrial fatty-acid oxidation by reversible enzyme deacetylation. *Nature*, *464*(7285), 121-125.

10. Borengasser SJ, Lau F, Kang P, Blackburn ML et al (2011). Maternal obesity during gestation impairs fatty acid oxidation and mitochondrial SIRT3 expression in rat offspring at weaning. *PLoS One*, *6*(8), e24068.

11. Kendrick AA, Choudhury M, Rahman SM, McCurdy CE, Friederich M et al (2011). Fatty liver is associated with reduced SIRT3 activity and mitochondrial protein hyperacetylation. *Biochemical Journal*, *433*(3), 505-514.

12. Hirschey, M. D. *et al.* SIRT3 regulates mitochondrial fatty-acid oxidation by reversible enzyme deacetylation. *Nature* 464, 121–125 (2010).

13. Qiu X, Brown K, Hirschey MD, Verdin E, Chen, D (2010) Calorie restriction reduces oxidative stress by SIRT3-mediated SOD2 activation. *Cell Metab.* 12, 662–667.

14. Someya S, Yu W, Hallows WC, Xu J, Vann JM, Leeuwenburgh C, et al. Sirt3 mediates reduction of oxidative damage and prevention of age-related hearing loss under caloric restriction. Cell. 2010 Nov 24;143(5):802-12.

15. Nassir, F., Adewole, O. L., Brunt, E. M., & Abumrad, N. A. (2013). CD36 deletion reduces VLDL secretion, modulates liver prostaglandins, and exacerbates hepatic steatosis in ob/ob mice. *Journal of lipid research*, *54*(11), 2988-2997.

16. Minehira K, Young SG, Villanueva CJ, Yetukuri L, Oresic M et al (2008). Blocking VLDL secretion causes hepatic steatosis but does not affect peripheral lipid stores or insulin sensitivity in mice. *Journal of lipid research*, *49*(9), 2038-2044.

17. Nassir F, Adewole OL, Brunt EM, Abumrad NA (2013). CD36 deletion reduces VLDL secretion, modulates liver prostaglandins, and exacerbates hepatic steatosis in ob/ob mice. *Journal of lipid research*, *54*(11), 2988-2997.

18. Charlton M, Sreekumar R, Rasmussen D, Lindor K, Nair KS (2002) Apolipoprotein Synthesis in Nonalcoholic Steatohepatitis. *Hepatology*. 35:4:898-904

19. Lett´eron P, Sutton A, Mansouri A, Fromenty B, Pessayre D (2003) Inhibition of Microsomal Triglyceride Transfer Protein: Another Mechanism for Drug-Induced Steatosis in Mice. *Hepatology*. 38:1:133-140

20. Jackson TK, Salhanick AI, Elovson J, Deichman ML, Amatruda JM. (1990). Insulin regulates apolipoprotein B turnover and phosphorylation in rat hepatocytes. *Journal of Clinical Investigation*, *86*(5), 1746.

21. Haas ME, Attie AD, Biddinger SB (2013). The regulation of ApoB metabolism by insulin. *Trends in Endocrinology & Metabolism*, *24*(8), 391-397.

22. Arrol S, Mackness M I, Durrington, PN (2000). The effects of fatty acids on apolipoprotein B secretion by human hepatoma cells (HEP G2). *Atherosclerosis*, *150*(2), 255-264.

23. Tietge UJ, Bakillah A, Maugeais C, Tsukamoto K, Hussain M, et al (1999). Hepatic overexpression of microsomal triglyceride transfer protein (MTP) results in increased in vivo secretion of VLDL triglycerides and apolipoprotein B. *Journal of lipid research*, *40*(11), 2134-2139.

24. Leung GK, Véniant MM, Kim SK, Zlot CH, Raabe, M (2000). A deficiency of microsomal triglyceride transfer protein reduces apolipoprotein B secretion. *Journal of Biological Chemistry*, *275*(11), 7515-7520.

25. Liao W, Hui TY, Young SG, Davis RA. (2003). Blocking microsomal triglyceride transfer protein interferes with apoB secretion without causing retention or stress in the ER. *Journal of lipid research*, *44*(5), 978-985.

26. Di Filippo M, Moulin P, Roy P, Samson-Bouma ME, Collardeau-Frachon S (2014). Homozygous MTTP and APOB mutations may lead to hepatic steatosis and fibrosis despite metabolic differences in congenital hypocholesterolemia. *Journal of hepatology*, *61*(4), 891-902.

27. Newberry EP, Xie Y, Kennedy SM, Luo J, Davidson NO (2006). Protection against Western diet–induced obesity and hepatic steatosis in liver fatty acid–binding protein knockout mice. *Hepatology*, *44*(5), 1191-1205.

28. Maeda N, Shimomura I, Kishida K, Nishizawa H, Matsuda M, et al(2002). Diet-induced insulin resistance in mice lacking adiponectin/ACRP30. *Nature medicine*, *8*(7), 731-737.

29. Huang W, Metlakunta A, Dedousis N, Zhang P, Sipula I et al (2010). Depletion of liver Kupffer cells prevents the development of diet-induced hepatic steatosis and insulin resistance. *diabetes*, *59*(2), 347-357.

30. Spruss A, Kanuri G, Wagnerberger S, Haub S, Bischoff SC et al (2009). Toll-like receptor 4 is involved in the development of fructose-induced hepatic steatosis in mice. *Hepatology*, *50*(4), 1094-1104.

31. Kovalovich K, DeAngelis RA, Li W, Furth EE, Ciliberto G et al (2000). Increased toxin-induced liver injury and fibrosis in interleukin-6–deficient mice. *Hepatology*, *31*(1), 149-159.

32. Amacher DE, Chalasani N (2014, May). Drug-induced hepatic steatosis. In *Seminars in liver disease* (Vol. 34, No. 02, pp. 205-214). Thieme Medical Publishers.

33. Browning JD, Horton JD (2004). Molecular mediators of hepatic steatosis and liver injury. *The Journal of clinical investigation*, *114*(2), 147-152.

34. Flores C, Adhami N, Martins-Green M (2016) THS Toxins Induce Hepatic Steatosis by Altering Oxidative Stress and SIRT1 Levels. J Clin Toxicol 6: 318.

35. Lindholm CR, Ertel RL, Bauwens JD, Schmuck EG, Mulligan JD et al (2013). A high-fat diet decreases AMPK activity in multiple tissues in the absence of

hyperglycemia or systemic inflammation in rats. *Journal of physiology and biochemistry*, 1-11.

36. Li SJ, Liu CH, Chang CW, Chu HP, Chen KJ et al (2015). Development of a dietary-induced metabolic syndrome model using miniature pigs involvement of AMPK and SIRT1. *European journal of clinical investigation*, *45*(1), 70-80.

37. Tateya S, Rizzo-De Leon N, Handa P, Cheng AM, Morgan-Stevenson V et al (2013). VASP increases hepatic fatty acid oxidation by activating AMPK in mice. *Diabetes*, *62*(6), 1913-1922.

38. Sun Y, Connors KE, Yang, D. Q. (2007). AICAR induces phosphorylation of AMPK in an ATM-dependent, LKB1-independent manner. *Molecular and cellular biochemistry*, *306*(1-2), 239-245.

39. Tomita K, Tamiya G, Ando S, Kitamura N, Koizumi H et al (2005). AICAR, an AMPK Activator, Has Protective Effects on Alcohol-Induced Fatty Liver in Rats. *Alcoholism: Clinical and Experimental Research*, *29* (s3).

40. Liu S, Jing F, Yu C, Gao L, Qin Y et al (2015). AICAR-induced activation of AMPK inhibits TSH/SREBP-2/HMGCR pathway in liver. *PloS one*, *10*(5), e0124951.

Figure 3.1. THS-exposure affects FA, TG and total lipid levels in the liver. Mice were exposed to THS toxins for six months before extracting the liver and serum for analysis (see Material and methods). THS-exposed mice have more (A) Free fatty acids in serum (B) TG in serum and (C) lipids in liver than control mice *= $p < 0.05$, ** $p<0.01$, ***$p< 0.0006$, NS= *Not statistically significant.* n=3 *P values were adjusted for the number of times each test was run.*

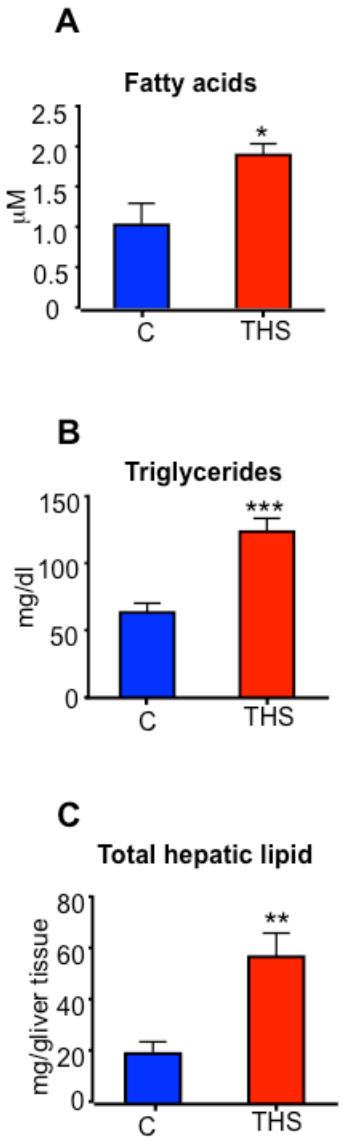
A
Fatty acids
2.5
2.0
1.5
1.0
0.5
0
µM
*
C
THS
B
Triglycerides
150
100
50
0
mg/dl
***
C
THS
C
Total hepatic lipid
80
60
40
20
0
mg/gliver tissue
**
C
THS

Figure 3.1

Figure 3.2. THS-exposure in conjunction Western Diet does not affects FA, TG and total lipid levels in the liver. THS-exposed mice placed on WD for five months before extracting the liver and serum for analysis (see Material and methods). THS-exposed mice placed on WD do not have a significant increase in (A) Free fatty acids, (B) TG levels, and (C) lipids compared to the THS-exposed mice on normal chow diet. *= $p< 0.05$, ** $p<0.01$, *NS= Not statistically significant.* n=3 *P values were adjusted for the number of times each test was run.*

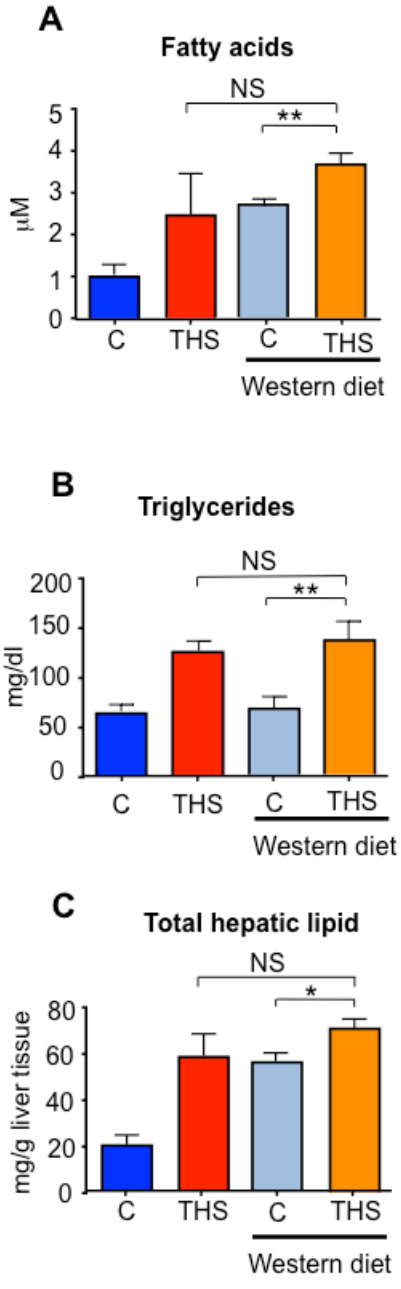
A
Fatty acids
NS
**
μM
5
4
3
2
1
0
C
THS
C
THS
Western diet
B
Triglycerides
NS
**
mg/dl
200
150
100
50
0
C
THS
C
THS
Western diet
C
Total hepatic lipid
NS
*
mg/g liver tissue
80
60
40
20
0
C
THS
C
THS
Western diet

Figure 3.2

Figure 3.3. THS-exposure in conjunction with AICAR treatment affects FA, TG and total lipid levels in the liver. THS-exposed mice treated with AICAR for eight weeks before the liver and serum was extracted for analysis. THS-exposed mice treated with AICAR have less (A) Free fatty acids (B) TG levels and (C) lipids than THS-exposed mice not treated with AICAR. *= $p< 0.05$, ** $p<0.01$, *NS= Not statistically significant.* n=3 *P values were adjusted for the number of times each test was run.*

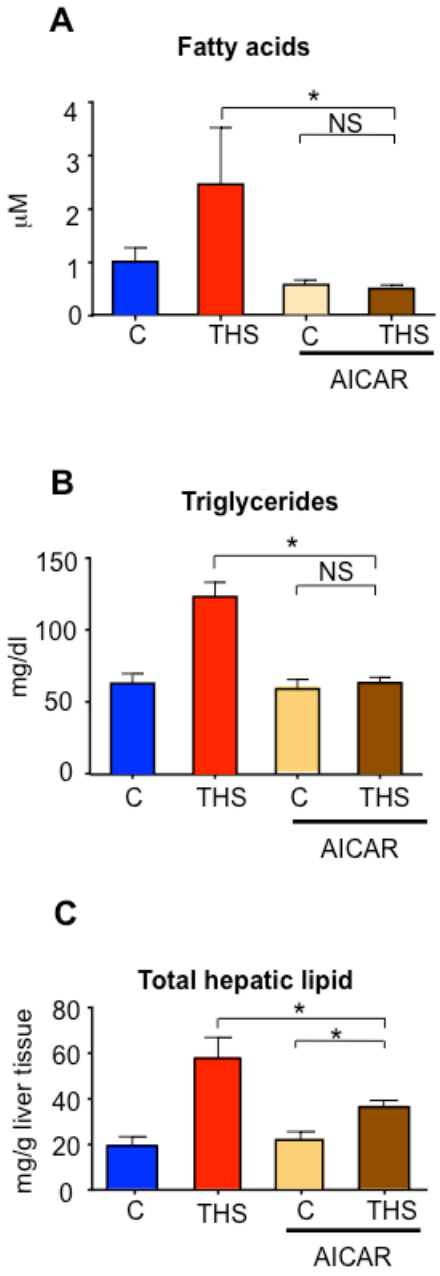
A
Fatty acids
μM
4
3
2
1
0
*
NS
C
THS
C
THS
AICAR
B
Triglycerides
mg/dl
150
100
50
0
*
NS
C
THS
C
THS
AICAR
C
Total hepatic lipid
mg/g liver tissue
80
60
40
20
0
*
*
C
THS
C
THS
AICAR

Figure 3.3

Figure 3.4. Effects of THS-exposure on the levels of enzymes involved in fatty acid metabolism. Mice were exposed to THS toxins for six months before extracting the liver for analysis of enzyme levels (see Material and methods). (A-B) THS-exposed mice also have no significant change in acetyl-coA carboxylase (ACC) and carnitine palmitoyltransferase I (CPT1). (C) THS-exposed mice do not have lower long-chain acyl-CoA dehydrogenases (LCAD) levels or lower isocitrate dehydrogenase 2 (IDH2) levels than controls (D). *= $p< 0.05$, ** $p<0.01$, *NS= Not statistically significant.* n=3 . *P values were adjusted for the number of times each test was run.*

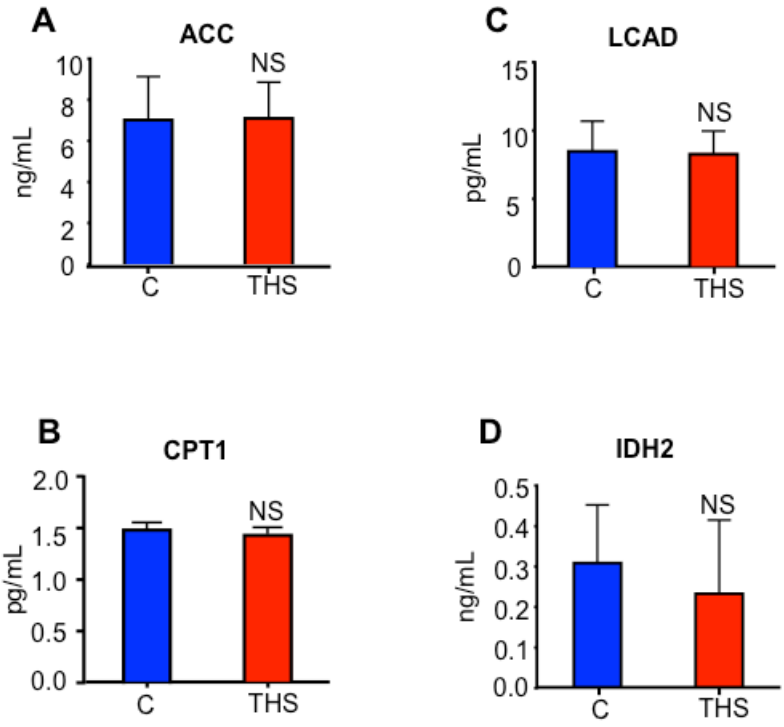
A
ACC
NS
ng/mL
10
8
6
4
2
0
C
THS
C
LCAD
15
10
5
0
pg/mL
NS
C
THS
B
CPT1
2.0
1.5
1.0
0.5
0.0
pg/mL
NS
C
THS
D
IDH2
0.5
0.4
0.3
0.2
0.1
0.0
ng/mL
NS
C
THS

Figure 3.4

Figure 3.5. THS toxins decrease IDH2 activity, SIRT3 and ATP levels in the lTHS-exposed mice. Mice were exposed to THS toxins for six months before extracting the liver for analysis of enzyme activity and levels (see Material and methods). (A) THS-exposed mice have lower IDH2 activity than control mice. (B) THS-exposed mice have lower SIRT3 levels and ATP levels (C) than control mice. *= $p< 0.05$, ** $p<0.01$ *NS*= *Not statistically significant.* n=10 for A and n=6 for B and C. *P values were adjusted for the number of times each test was run.*

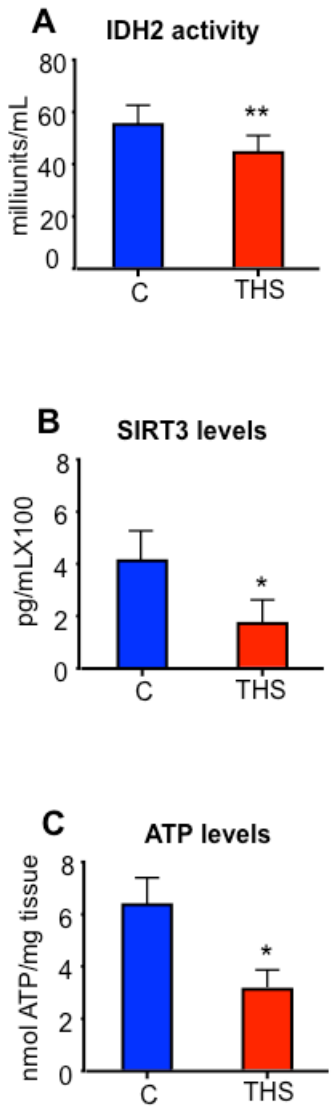
A
IDH2 activity
milliunits/mL
80
60
40
20
0
**
C
THS
B
SIRT3 levels
pg/mLX100
8
6
4
2
0
*
C
THS
C
ATP levels
nmol ATP/mg tissue
8
6
4
2
0
*
C
THS

Figure 3.5

Figure 3.6. THS exposure results in a decrease of VLDL assembly in the liver. Mice were exposed to THS toxins for six months before extracting the liver for analysis of enzyme levels (see Material and methods). (A) THS-exposed mice have lower levels of apoB in the liver than control mice. (B) THS toxins also result in lower MTTP protein in the liver of THS-exposed mice. (C) Lastly, THS-exposed mice also have lower levels of VLDL in the liver compared to the control mice. *= $p < 0.05$, ** $p<0.01$, ***$p < 0.0006$, *NS= Not statistically significant.* n=6 *P values were adjusted for the number of times each test was run.*

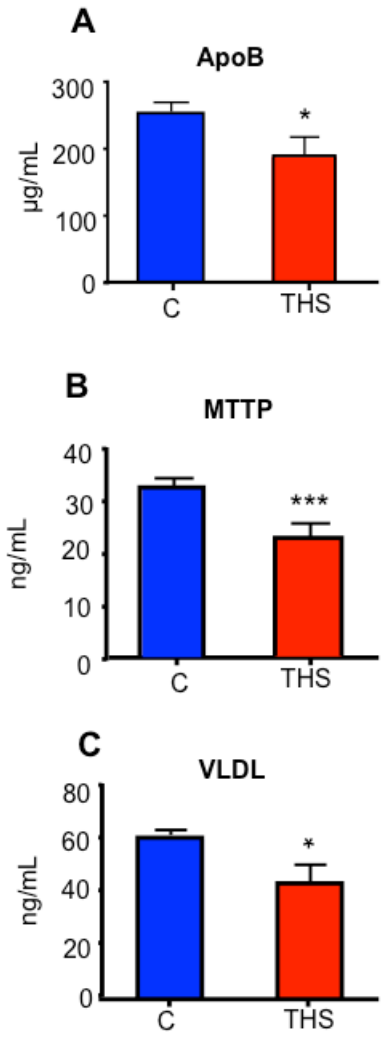
A
ApoB
300
200
100
0
µg/mL
*
C
THS
B
MTTP
40
30
20
10
0
ng/mL
***
C
THS
C
VLDL
80
60
40
20
0
ng/mL
*
C
THS

Figure 3.6

Figure 3.7. Plausible mechanism of how THS toxins alter VLDL assembly and fatty acid breakdown in the liver resulting in THS-induced hepatic steatosis. (A) THS decreases apoB resulting in TG accumulation in the liver (B) In addition to low levels of VLDL particles, THS-exposed mice also have lower fatty acid breakdown. THS-exposed mice have lower levels of SIRT3 and lower IDH2 activity and consequently lower fatty acid breakdown. Low levels VLDL and fatty acid breakdown lead to increase lipid accumulation in the liver and consequently development of THS-induced hepatic steatosis.

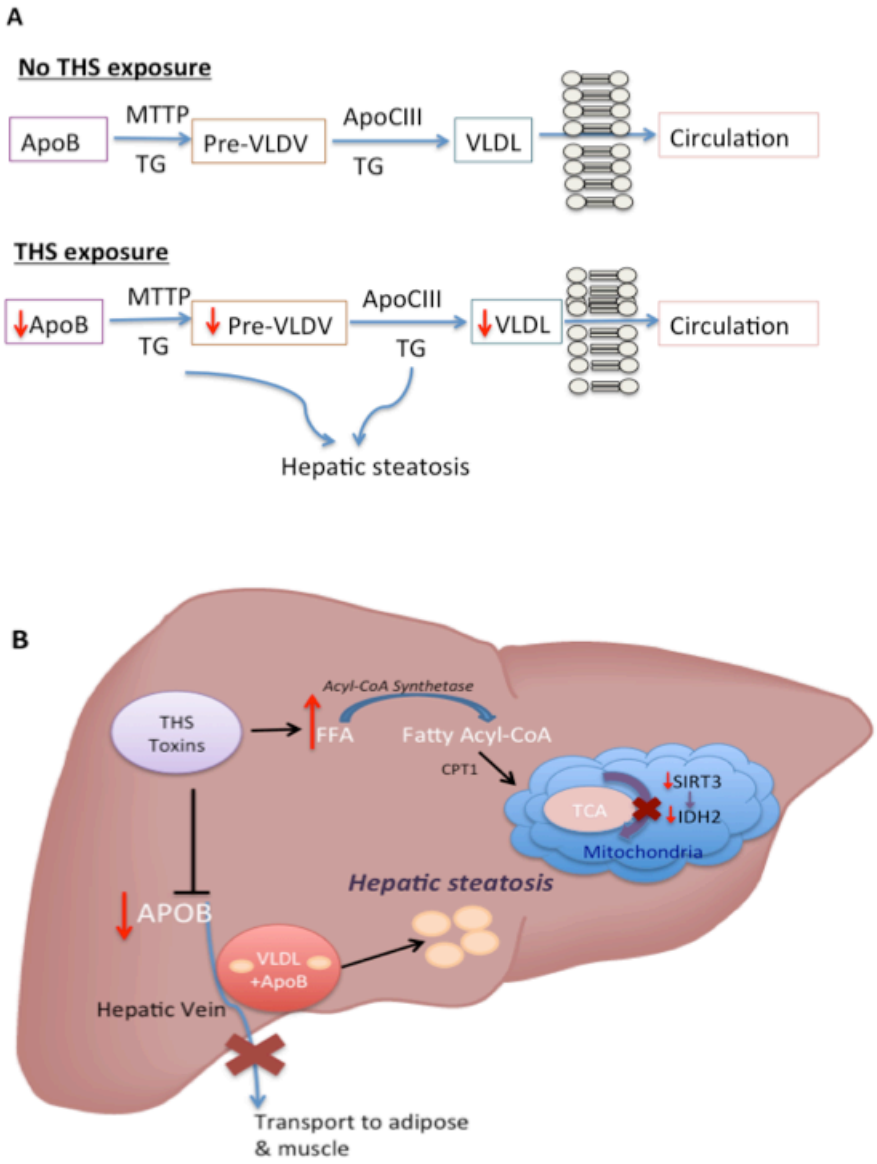
A
No THS exposure
ApoB
MTTP
TG
Pre-VLDV
ApoCIII
TG
VLDL
Circulation
THS exposure
ApoB
MTTP
TG
Pre-VLDV
ApoCIII
TG
VLDL
Circulation
Hepatic steatosis
B
THS Toxins
Acyl-CoA Synthetase
FFA
Fatty Acyl-CoA
CPT1
SIRT3
IDH2
TCA
Mitochondria
Hepatic steatosis
APOB
VLDL +ApoB
Hepatic Vein
Transport to adipose & muscle

Figure 3.7

CHAPTER 4: Conclusion

The liver performs multiple metabolic functions and therefore compromising this organ can lead to the development of various diseases. Multiple non-genetic factors such as toxins, drugs, and diet can result in hepatic steatosis. To date, there is no treatment for hepatic steatosis and if is not detected and treated early it can progress to fibrosis, cirrhosis and hepatic carcinoma. A healthy lifestyle and cessation of exposure to toxins or drugs appears to be the key in reversing lipid accumulation in the liver and preventing hepatic steatosis. Evidence about the toxicity of THS toxins has been accumulating over the past years, however, not many studies have focused in the molecular and cellular damage of chronic exposure to this form of tobacco toxins. Moreover, virtually nothing is known about the molecular and cellular mechanism underlying the development of THS-induced hepatic steatosis.

I have provided a molecular and cellular mechanism of THS-induced hepatic steatosis in mice. I show that THS toxins lead to an increase oxidative stress in the liver resulting in THS-induce hepatic steatosis. THS-exposed mice have higher levels of oxidative-stress-mediated damage and more lipid accumulation in the liver. More importantly, when the THS-exposed mice were treated with antioxidants some of the cellular and molecular damage was reversed and the accumulation of lipids was decreased, suggesting that the damaging effects of THS toxins are mediated by a redox imbalance in these animals. Conversely, when THS-exposed mice were treated with APAP (Tylenol), oxidative stress increased as well as the accumulation of lipids.

I also show that exposure to THS toxins results in lower fatty acid metabolism and VLDL assembly. Treatment with AICAR, which is a common diabetes treatment, decreased fat accumulation in THS-exposed mice. THS-exposed mice have higher levels of fatty acids and TG and they were unable to process fatty acids by the TCA cycle. THS-exposed mice also have decreased VLDL assembly suggesting that the excess amount of lipids is not being transported out of the liver.

The findings presented here are novel and innovative because we (a) used a novel THS animal exposure system that mimics human exposure to THS in everyday life and (b) elucidated cellular and molecular mechanisms of lipid accumulation in the liver due to long-term THS exposure using mice as a model system. Virtually no exposure systems have been developed prior to the one proposed here for *in vivo* studies and the dangers of THS in the liver have also not been studied yet. As a consequence, these findings provide the basis and a model to study the adverse effects of THS toxins in the liver. They provide the basis for understanding the effects of THS toxins in the liver and they add to the accumulated evidence of the toxicity of THS. Additional studies need to be done to investigate whether, in addition to hepatic steatosis, exposure to toxins can lead to other diseases affecting the liver such as cancer and hepatitis.

Finally, the impact of the studies showed here is two fold: (a) They elucidate the mechanism by which THS-induced hepatic steatosis occurs so better treatments can be designed and (b) they will lead to studies in humans, which can then result in policymaking aimed at reducing exposure to THS toxins.